Nanoscale Horizons

ROYAL SOCIETY OF CHEMISTRY

REVIEW

View Article Online
View Journal | View Issue

Cite this: *Nanoscale Horiz.*, 2023, **8**, 422

pH-Responsive wound dressings: advances and prospects

Zeyu Han,†[ab] Mujie Yuan,†[ab] Lubin Liu,[b] Kaiyue Zhang,[ab] Baodong Zhao,[ab] Bin He,[c] Yan Liang *[d] and Fan Li *[ab]

Received 11th December 2022,
Accepted 31st January 2023

DOI: 10.1039/d2nh00574c

rsc.li/nanoscale-horizons

Wound healing is a complex and dynamic process, in which the pH value plays an important role in reflecting the wound status. Wound dressings are materials that are able to accelerate the healing process. Among the multifunctional advanced wound dressings developed in recent years, pH-responsive wound dressings, especially hydrogels, show great potential owing to their unique properties of adjusting their functions according to the wound conditions, thereby allowing the wound to heal in a regulated manner. However, a comprehensive review of pH-responsive wound dressings is lacking. This review summarizes the design strategies and advanced functions of pH-responsive hydrogel wound dressings, including their excellent antibacterial properties and significant pro-healing abilities. Other advanced pH-responsive materials, such as nanofibers, composite films, nanoparticle clusters, and microneedles, are also classified and discussed. Next, the pH-monitoring functions of pH-responsive wound dressings and the related pH indicators are summarized in detail. Finally, the achievements, challenges, and future development trends of pH-responsive wound dressings are discussed.

1. Introduction

The skin is a human organ that is in direct contact with the external environment. Its functions of temperature regulation and the sensing of external stimuli are significant for protecting the body from external damage.[1–3] Skin injuries are one of the most common types of injuries in the human body, causing pain and discomfort, and even death.[4–6] After injury, wound healing is a dynamic and complex process that is usually divided into four phases: hemostasis, inflammation, proliferation, and remodeling (Fig. 1).[7–9] The healing process is disturbed by adverse effects occurring at any stage, such as infections, inflammation, diabetes, pH, and temperature[10–13]

Wound dressings act as barriers to cover wounds and reduce the risk of infection.[14] In recent years, hydrogels,[15] electrospun films,[16] sponges,[17] and other novel wound dressings have been developed. Compared with traditional wound dressings, they have more advanced functions to promote wound healing, such as inhibiting bacterial growth, maintaining moisture retention, absorbing exudate, and releasing drugs.[18,19] However, several new ideas in wound dressings are to be explored further. The process of wound healing is dynamic; therefore, the function of wound dressings is to be regulated according to wound status.[20] Furthermore, progress should be made in the fields of wound-status clarification and warning of infection risks.[21]

pH-Responsive wound dressings provide solutions to the aforementioned issues since the pH of the skin is closely related to the wound healing process. The pH of healthy skin is between 4 and 6 due to the products of fatty acids and amino acids secreted by keratinocytes, which provides a slightly acidic environment to inhibit bacterial proliferation.[22] Generally, wounds are classified as acute wounds (wounds that heal in an orderly and timely manner and result in sustained restoration of anatomic and functional integrity) and chronic wounds (wounds that fail to heal through an orderly and timely process to achieve anatomic and functional integrity). When acute wounds occur, internal tissue and interstitial fluid with a pH of approximately 7.4 was exposed, changing the acidic milieu of normal skin, and the pH will return to acidic as wound healing. Chronic wounds have a pH between 7 and 9 because of the existence of blood, interstitial fluid, ammonia, *etc.*[23] In addition, when bacterial infection occurs in a wound, the pH of the wound will decrease due to the acidic substances such as lactic acid and carbonic acid generated by bacterial growth.[24] Therefore, pH is considered a reliable indicator of the wound status, and the

[a] *Department of Oral Implantology, The Affiliated Hospital of Qingdao University, Qingdao 266000, China. E-mail: lifan911017@qdu.edu.cn*
[b] *School of Stomatology, Qingdao University, Qingdao 266000, China*
[c] *National Engineering Research Center for Biomaterials, Sichuan University, Chengdu 610064, China*
[d] *Department of Pharmaceutics, School of Pharmacy, Qingdao University, Qingdao 266000, China. E-mail: liangyan072@foxmail.com*
† These authors contributed equally in this work.

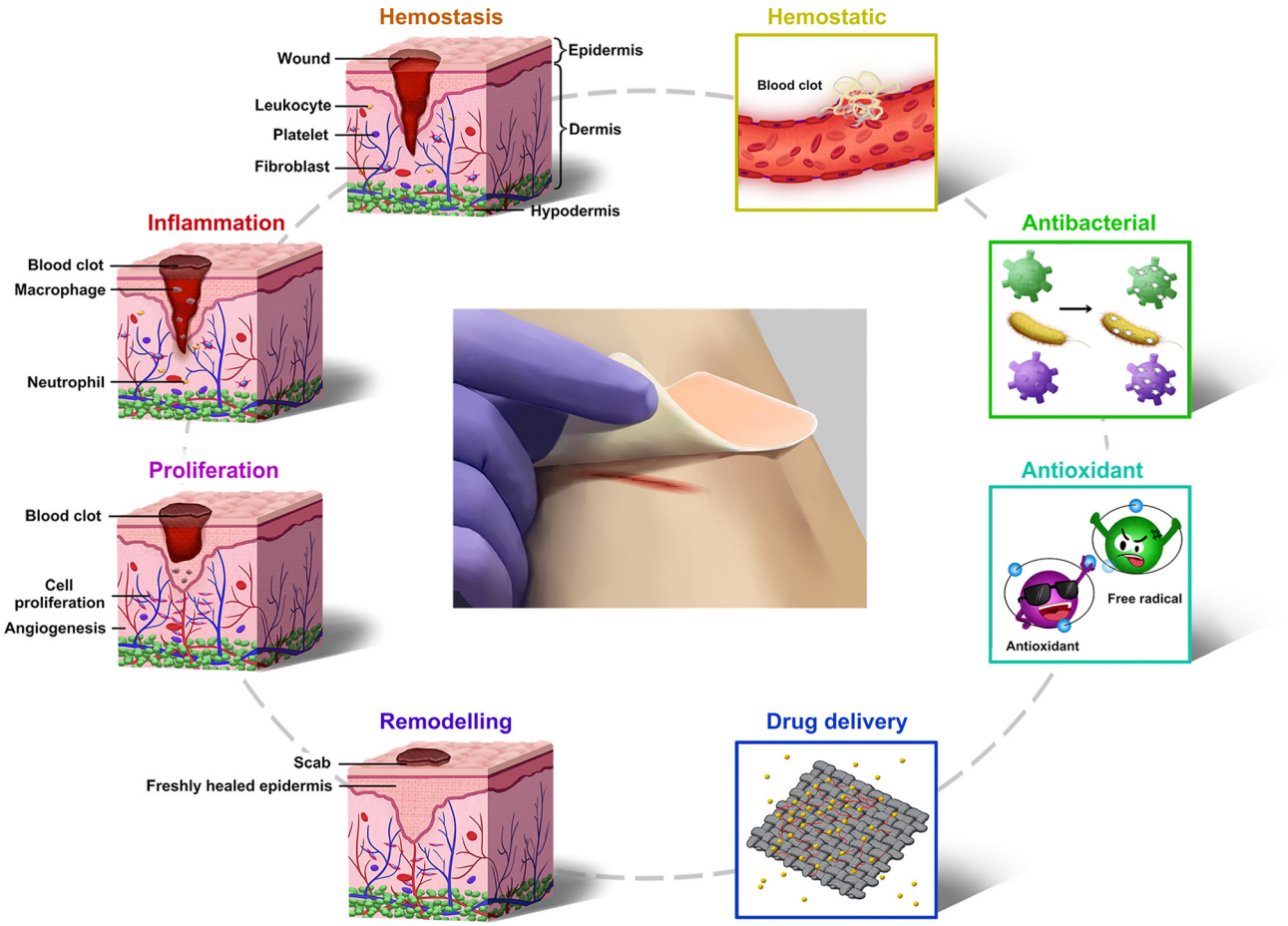

Fig. 1 Schematic of the four stages of wound healing and the main advanced functions of pH-responsive wound dressings.

variation in pH predicts a tendency for wound healing/deterioration.[25] It is to be noted that pH-responsive wound dressings have unparalleled advantages in wound care because of their excellent biochemical and mechanical properties and their ability to tune their morphology,[26] volume,[27] and drug release behavior.[28] Such materials are able to monitor the wound status based on the pH of the wound, heal the wound in a controlled way, reduce the infection risks, and shorten the healing time. However, a systematic review of the pH-responsive wound dressings still has not been reported.

In this article, a comprehensive overview of pH-responsive wound dressings, from the most common and widely used hydrogel to other wound dressings is presented, showing their characteristics and advantages for wound healing (Fig. 1). The article begins by providing the design strategies and advanced functions of pH-responsive hydrogel wound dressings. Other types of pH-responsive wound dressings are then classified and discussed, including nanofibers, composite films, nanoparticle clusters, microneedles, *etc.* A detailed summary of the pH-monitoring functions of pH-responsive wound dressings and related pH indicators follows. Finally, the review is concluded with a discussion on the challenges and future development trends of pH-responsive wound dressings.

2. pH-Responsive hydrogel wound dressings

2.1. Design strategies for pH-responsive hydrogel wound dressings

pH-Responsive hydrogel wound dressings are able to receive changes in the pH of the local environment of the wound and adjust their functions to meet the needs of wound healing.[20] In this section, we briefly summarize the design strategies for pH-responsive hydrogel wound dressings, which are mainly classified into pH-responsive morphology, size, degradation, and drug release behavior (Fig. 2).

pH-Responsive morphology implies that under specific conditions, the morphological properties of the dressings are functional or nonfunctional (Fig. 2(a)). When replacing wound dressings, the adhesion between the dressing and wound often causes pain and even secondary injury to the wound.[14] The liquid-to-solid reversible morphological conversion of hydrogels has a unique effect in solving this problem, and this type of response is usually designed through imine bonds, Schiff-base bonds, and catechol–Fe coordinate bonds.[26,29–32] For instance, Liang *et al.* developed hydrogels with excellent pro-healing and on-demand dissolution or removal properties *via* dual-dynamic-bond cross-linking of catechol–Fe coordinate bond and dynamic

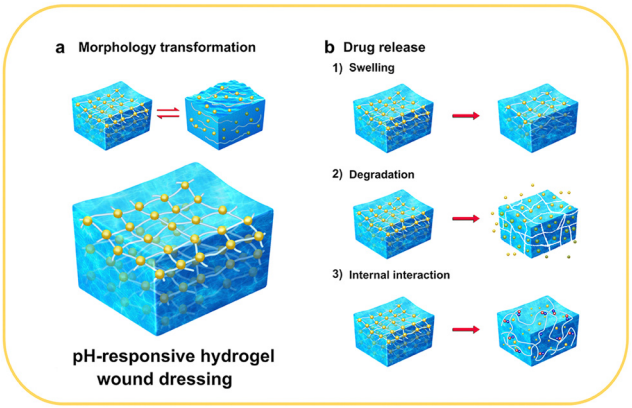

Fig. 2 The design strategies for pH-responsive hydrogel wound dressings.

Schiff base bonds. After the treatment, the adhesive force of the dressing can be significantly reduced with the intervention of acid solution or deferoxamine mesylate solution, thereby easily removing the dressing and reducing patient suffering and the risk of unnecessary injury.[32]

Changes in the pH-responsive size mainly refer to the swelling behavior of the hydrogels. The swelling ratios of hydrogels vary significantly with pH, causing a change in the pore size inside the materials that perform pH-responsive drug delivery or signal transmission (Fig. 2(b1)). The different swelling behaviors are generally attributed to protonation, deprotonation, and charge repulsion of the functional groups in the material components.[33–35] For example, pH-sensitive composite hydrogels prepared by Al-Arjan *et al.* showed a high curcumin release at pH 7.4. At this pH, the hydrophilic groups on bacterial cellulose (BC), polyvinyl alcohol (PVA), and graphene oxide (GO) caused swelling owing to hydrogen bonds and electrostatic repulsion forces.[36]

pH-Responsive degradation is an effective strategy for controlling drug release (Fig. 2(b2)). Ideally, when bacteria proliferate, pH-responsive degradation occurs, and then the drug is released to kill the bacteria. When the pH of the wound area returns to normal, the degradation process is terminated. The strength of the three-dimensional network of the hydrogels is weakened with an increase in the degradation rate, leading to larger internal pore size. For example, methylcellulose-based hydrogel prepared by Bonetti was crosslinked by ester bonds, and ester bonds would hydrolyze in an alkaline environment, which leads to hydrogel network expansion and drug release.[37] In addition, the degradation of the loaded nanoparticles contributes to the pH-responsive behavior. The hydrogel–microgel composite prepared by Du *et al.* displayed elevated drug release owing to the higher degradation rate of the hydrogel networks.[38] This method has also been reported in other studies on pH-responsive hydrogel wound dressings.[39–41]

pH-Responsive drug release is the ultimate goal of most pH-responsive hydrogel wound dressings. In addition to the aforementioned swelling and degradation behaviors, the pH-responsiveness is also influenced by other factors, such as the type of medium, concentration of ions in the medium, and interactions between drugs and the other components (Fig. 2(b3)).[34,42,43] Therefore, the influence of various factors should be carefully considered when designing pH-responsive and controlled drug release systems. Furthermore, the sensitivity of pH-responsiveness must be examined in conditions that simulate the wound environment to ensure its applicability. A summary of the types, applications, synthetic methods, pH response mechanisms, and other relevant information about pH-responsive hydrogel wound dressings is presented in Table 1.

2.2. Advanced properties of pH-responsive hydrogel wound dressings

Hydrogels are three-dimensional networks formed by the physical or chemical cross-linking of hydrophilic polymers.[19] These are widely used in wound dressings because of their ability to maintain the cleanliness and wettability of wounds, thereby preventing infections and promoting wound healing.[69] In addition, hydrogels are excellent carriers for loading cells, antimicrobials, growth factors, and biological macromolecules.[30,50,64] pH-Responsive hydrogels play an important role in wound regeneration. Depending on composition, hydrogels are able to change their morphology, swelling behavior, degradation, or drug delivery efficiency based on the variation in pH; therefore, the wound healing process could be better regulated.[26,45,60] In this section, we discuss recent advances in pH-responsive hydrogel wound dressings from the perspective of function.

2.2.1. pH-Responsive antibacterial hydrogel wound dressings. Bacterial infection is the most common and unavoidable issue in wound healing. Bacterial infections can cause inflammatory reactions around the wound and delay healing. Moreover, severe infections can lead to life-threatening complications, such as sepsis, shock, organ failure, *etc.*[70–72] Therefore, the inhibition of bacterial infection is an effective means to promote wound healing and prevent complications. The antibacterial mechanisms of pH-responsive antibacterial hydrogel wound dressings were elaborated and summarized (Fig. 3).

2.2.1.1. Delivery of synthetic antimicrobial agents. The use of antibiotics is the most common and effective strategy to treat wound infections in clinics.[73] In recent years, a large number of antibiotics have been encapsulated in hydrogels to prevent infections, such as aminoglycosides,[74] novobiocin,[75] vancomycin, gentamicin, and minocycline.[76] pH-Responsive hydrogels could accurately regulate the release behavior to achieve controlled and sustained release of antibiotics. Hosseini and Mohammad synthesized a hydrogel film based on basil seed mucilage and using various ratios of PVA, glutaraldehyde as a cross-linker, and glycerol as a plasticizer. The hydrogel film demonstrated excellent control over the release of antibiotics. The release efficiency of tetracycline hydrochloride (TH) was approximately 80% under alkaline conditions (pH 7.4/8.5, 120 h). However, under acidic conditions (pH 6.5, 120 h), the migration of TH from the TH-loaded film was difficult, and the drug release rate was only 46.5%.[44] The design of the hydrogel membrane can adjust the release process and amount of TH according to the wound conditions, making the use of antibiotics more intelligent.

Table 1 Summary of pH-responsive hydrogel wound dressings

Application	Composition	Synthetic methods	pH range	pH-Responsive mechanism	Ref.
Delivery of antibiotic: tetracycline hydrochloride (TH)	PVA, glutaraldehyde, glycerol	Chemical crosslinking	Higher release at basic conditions	Ionization of the hydroxyl and carboxyl groups	44
Delivery of antibacterial agent: triclosan	Peptide-based bis-acrylate, acrylic acid	Radical polymerization	Higher swelling ratios at basic conditions	Hydrogen bonds break in neutral or basic conditions	45
Delivery of antibiotic: gentamycin sulphate	Chitosan (CS), PVP, glycerol, PNIPAm	Chemical crosslinking	Higher swelling ratios at acidic conditions	Deprotonation of the $-NH_2$ group and –NH group	27
Delivery of antibiotic: silver-sulphadiazine	Arabinoxylan, CS, reduced graphene oxide, tetraethyl orthosilicate	Chemical crosslinking	Higher swelling ratios at neutral conditions	The alcoholic and carboxylic acid functional groups at acidic conditions, the influence of Na^+ at basic conditions	43
Delivery of antibiotic: silver-sulphadiazine	Arabinoxylan, carrageenan, reduced graphene oxide, tetraethyl orthosilicate	Chemical crosslinking	Higher swelling ratios at neutral conditions	The alcoholic and carboxylic acid functional groups at acidic conditions, the influence of Na^+ at basic conditions	46
Delivery of antibiotic: silver-sulphadiazine	Carboxymethyl chitosan, oxidized carboxymethyl cellulose	Schiff-base reaction	Higher release at pH 5.5 and pH 9.5	The stronger degradation rate in acid and intensive electrostatic repulsion in alkali	38
Release of tobramycin and borneol	Dialdehyde carboxymethyl cellulose, tobramycin, β-cyclodextrin derivative	Chemical crosslinking	High degradation at acidic conditions	Gradual hydrolysis of the imine bond in a weakly acidic environment	39
Release of graphene oxide quantum dots	Tannic acid, keratin	Chemical crosslinking	Higher swelling ratios at neutral alkaline conditions	High deprotonation and repulsion between the acidic chains in basic solutions	47
Release of AgNPs	Methylcellulose, citric acid	Chemical crosslinking	High degradation at alkaline conditions	Network expansion and release of AgNPs were due to the alkaline hydrolysis of ester bonds	37
Release of antibiotic and ZnS nanoparticles	2-(Dimethylamino)ethyl methacrylate/polyethylene oxide, ZnS nanoparticles	γ-Irradiation polymerization	Higher swelling ratios at pH 4–7	Decrease of protonation and intermolecular hydrogen bonds lead to a high swelling ratio (pH 4–7)	34
Release of silver nanoparticles (AgNPs) and deferoxamine	Oxidized dextran, dopamine	Schiff-base reaction	Higher degradation at acidic conditions	Gradually destroyed network at acidic conditions	48
Release of antibiotic and lysozyme	Gelatin methacryloyl, hyaluronic acid-aldehyde	Photo-crosslinking	High release at acidic conditions	The breakage of Schiff base bonds and the electrostatic interaction.	49
Release of antibiotic and basic fibroblast growth factor (bFGF)	Alginate, $CaCO_3$ microparticles	Microfluidic technology	Slower release rate at pH 6.4	Presence of $CaCO_3$ and strong interactions between $CaCO_3$ microspheres and the alginate network	50
Release of antibiotic	Silica nanoparticles, alginates	Chemical crosslinking	High release at alkaline conditions	The degradation of silica nanoparticles	51
Release of natural antibacterial substance: honey	PVA, chitosan, montmorillonite	Freezing–thawing method	Lower swelling ratios at acidic conditions	Protonation of amine groups to NH_3^+ at acidic conditions	52
Release of natural antibacterial substance: resveratrol	Poly(vinylalcohol)-borax (PB), resveratrol grafted cellulose nanofibrils (RPC)	Crosslinked by dynamic borate bonds and hydrogen bonds	Higher release at acidic conditions	Faster degradation of RPC/PB hydrogels at acidic conditions	40
Release of natural antibacterial substance: curcumin	Quaternized chitosan (QCS), benzaldehyde-terminated Pluronic®F127	Chemical crosslinking	Higher release at acidic conditions	Faster degradation of QCS/PF hydrogels at acidic conditions	41
Release of natural antibacterial substance: curcumin	Polyaspartic acid crosslinked by graphene nanosheets, poly(acrylamide-*co*-acrylic acid), copper oxide, zinc oxide nanoparticles	Chemical crosslinking	Low release at pH 2.1.	Compressed hydrogel network at pH 2.1	53
Release of natural antibacterial substance: curcumin	Blending bacterial nanocellulose, GO, PVA	Chemical crosslinking	Higher release at pH 7.4	Hydrophilic groups and more electrostatic repulsion forces	36
Release of natural antibacterial substance: curcumin	Methacrylated gelatin, methacrylated pectin	Photo-crosslinking	Higher release at pH 7.4	The ionization of carboxyl groups both in pectin and gelatin	54

Table 1 (*continued*)

Application	Composition	Synthetic methods	pH range	pH-Responsive mechanism	Ref.
Release of natural antibacterial substance: tannic acid (TA)	Carboxylated agarose, TA, zinc salts	Chemical crosslinking	Higher release at acidic conditions	Disruption of ionic interactions and protonation	55
Release of natural antibacterial substance: TA	Hydroxypropyl chitin, tannic acid, ferric ion	Chemical crosslinking	Higher release at acidic conditions	Stronger complexation due to the deprotonation of pyrogallol/catechol groups	56
Release of natural antibacterial substance: TA	Tannin–europium coordination complex, Eu^{3+}	Chemical crosslinking	Sustained release at acidic conditions	The metal–phenolic coordination and the protonation of phenolic hydroxyl groups	57
Release of natural antibacterial substance: TA	Gelatin (GTU), TA	One-pot physical hydrogen bonding	Higher release at high pH	Deprotonation of polymer and charge repulsion	58
Release of natural antibacterial substance: magnolol	Carboxyl-bearing magnolol derivative, chitosan hydrochloride	Chemical crosslinking	Higher release at acidic conditions	High degradation rate of magnolol-loaded chitosan nanocapsules at acidic conditions	59
Inherent antibacterial properties derived from CS	CS, PVA, guar gum, tetraethyl orthosilicate	Chemical crosslinking	Higher swelling at acidic conditions	Protonation of cationic groups, mainly $-NH_3$	33
Inherent antibacterial properties derived from CS	Collagen, CS, dialdehyde-terminated polyethylene glycol	Crosslinking by dynamic imine bonds	Sol state at acidic environment and hydrogel state at basic conditions.	Formation and breakage of imine linkages	26
Inherent antibacterial properties derived from Schiff-base bonds	Tetrabenzaldehyde-functionalized pentaerythritol, CS	Schiff-base reaction and hydrogen linkages	Sol state at acidic environment and hydrogel state at basic conditions	Hydration of hydrogen bonds and the dissociation of Schiff bases	29
Bacterial trap behavior and Fenton reaction	*N*-Isopropyl acrylamide, acrylamide, *N*-[3-(dimethylamino)propyl]methacrylamide	Free-radical polymerization and electrostatic adsorption	In acidic conditions, CP@Tf-hy shows *in situ* self-supplied H_2O_2 and pH-responsive release of Fenton catalytic copper ions with $^{\bullet}OH$	Intrinsic properties of CP@Tf	60
Photothermal therapy	Poly(glycerol sebacate)-*co*-poly(ethylene glycol)-*g*-catechol prepolymer 2 (PEGSD2), $FeCl_3$, GTU	Physical double-network linkages: catechol Fe^{3+} coordination and hydrogen bonding	Sol state at acidic environment	—	31
Photothermal therapy	Oxidized hyaluronic acid, QCS, berberine, epidermal growth factor, poly(styrene sulfonate)	Schiff-base reaction	Higher release at high pH	The protonation of the carboxyl group of oxidized hyaluronic acid	61
Photothermal therapy and pro-healing effect	Ferric iron, protocatechualdehyde containing catechol and aldehyde groups, QCS	Catechol–Fe coordinate bond and Schiff base bonds	Low adhesion at acid solution or deferoxamine mesylate solution	Catechol–Fe coordinate bond and Schiff base bonds	32
Enhance the resistance to bacteria	PVA, CMC, polyethylene glycol (PEG)	Freeze–thaw process and phase separation method	High swelling ratios at neutral conditions	Degree of dissociation of carboxylic groups	62
Release of the anti-inflammatory drug: diclofenac sodium	PVA, alginate-*g*-*N*-isopropyl acrylamide	Freeze thaw technique	High swelling ratios at neutral conditions	Repulsive interaction between the carboxyl group of alginate and diclofenac	63
Release of anti-inflammatory bioactive factors: SCF	Collagen, aldehyde polyethylene	Condensation between the primary amines of collagen and aldehydes of APG	Reversible morphological changes at acidic/basic conditions	Formation and breakage of imine linkages	30
Release of DNA-bearing polyplex	PEG, poly(sulfamethazine ester urethane) (PSMEU)	Physically crosslinking	Sol state at high pH and room temperature and gel state at the body conditions	Ionized sulfonamide groups	64
Release of anti-inflammatory drug: resolvin D1	Cystamine, *N*,*N*0-bis(a-cryloyl)cystamine, acetalized cyclodextrin	Double-network crosslinking	Higher release at low pH	The pH-responsiveness of acetalized cyclodextrin nanoparticles	65
Release of the anti-inflammatory drug: insulin	*N*-Carboxyethyl chitosan, hyaluronic acid-aldehyde, adipic acid dihydrazide	Chemical crosslinking	Faster degradation rate at acidic conditions	Labile acylhydrazone bonds at acidic pH	66
					67

Table 1 (*continued*)

Application	Composition	Synthetic methods	pH range	pH-Responsive mechanism	Ref.
Release of insulin and fibroblasts	Phenylboronic-modified chitosan, polyvinyl alcohol, benzaldehyde-capped polyethylene glycol	Cross-linking of Schiff's base and phenyl boronate ester	Higher release at acidic and glucose conditions	Unstable Schiff's base at acidic conditions. Preferred combination between the phenylboronic group and glucose over the hydroxyl group of PVA	
Release of the metformin and GO	Dihydrocaffeic acid and L-arginine cografted chitosan, phenylboronic acid and benzal-dehyde bifunctional polyethylene glycol-*co*-poly(glycerol sebacic acid), polydopamine-coated reduced graphene oxide	Double dynamic bond of the Schiff-base and phenylboronate ester	Higher release at acidic and glucose conditions	Unstable Schiff's base at acidic conditions. Phenylboronate ester structure with a phenylboronic acid group is glucose-responsive	68
Release of tobramycin	QCS, oxidized dextran, tobramycin, polydopamine-coated polypyrrole nanowires	Schiff-base reaction	Higher release at acidic conditions	Unstable Schiff's base at acidic conditions	24

Similarly, Zhu *et al.* synthesized a hydrogel that released an antimicrobial agent (triclosan) more rapidly in neutral or alkaline environments. In addition, the hydrogel can be biodegraded by enzymes owing to the presence of peptidic bonds.[45] Temperature- and pH-responsive gentamycin sulfate-loaded chitosan-based hydrogel films constructed by Mohammad and Fehmeeda showed better antibacterial activity at high pH and temperature because of the higher release of gentamycin sulfate.[27] Furthermore, the use of pH-responsive hydrogels as drug delivery systems can improve the bioavailability antimicrobials that are poorly water-soluble. For example, silver sulfadiazine is widely used for the treatment of various wounds, but its application is limited by its poor solubility in aqueous solutions.[38] Khan *et al.* addressed this problem by building a pH-responsive hydrogel (composed of arabinoxylan, CS, reduced graphene oxide, tetraethyl orthosilicate) to load silver sulfadiazine and control its release. The controlled and sustained release of silver sulfadiazine was achieved, with release rates of 93.1, 58.3, and 53.71% at pH 7.4, 6.4, and 8.4, respectively. This controlled drug release system successfully enhanced the bioavailability of silver sulfadiazine.[43] Their other study also reached similar conclusions by replacing CS with carrageenan.[46] Delivering antibiotics is an effective strategy for pH-responsive wound dressings, but only using antibiotics to fight bacterial infections may not be enough in some cases.

In addition to delivering antibiotics only, other adjuvant drugs or antibacterial materials can also be encapsulated in hydrogels to enhance their ability to fight infections. For example, in a study by Fan *et al.*, tobramycin was not directly encapsulated in hydrogels but was used as a cross-linking agent to react with carboxymethyl cellulose to form a hydrogel (the linking was designed through imine bonds, which gradually hydrolyze in a weakly acidic environment). The use of tobramycin as a cross-

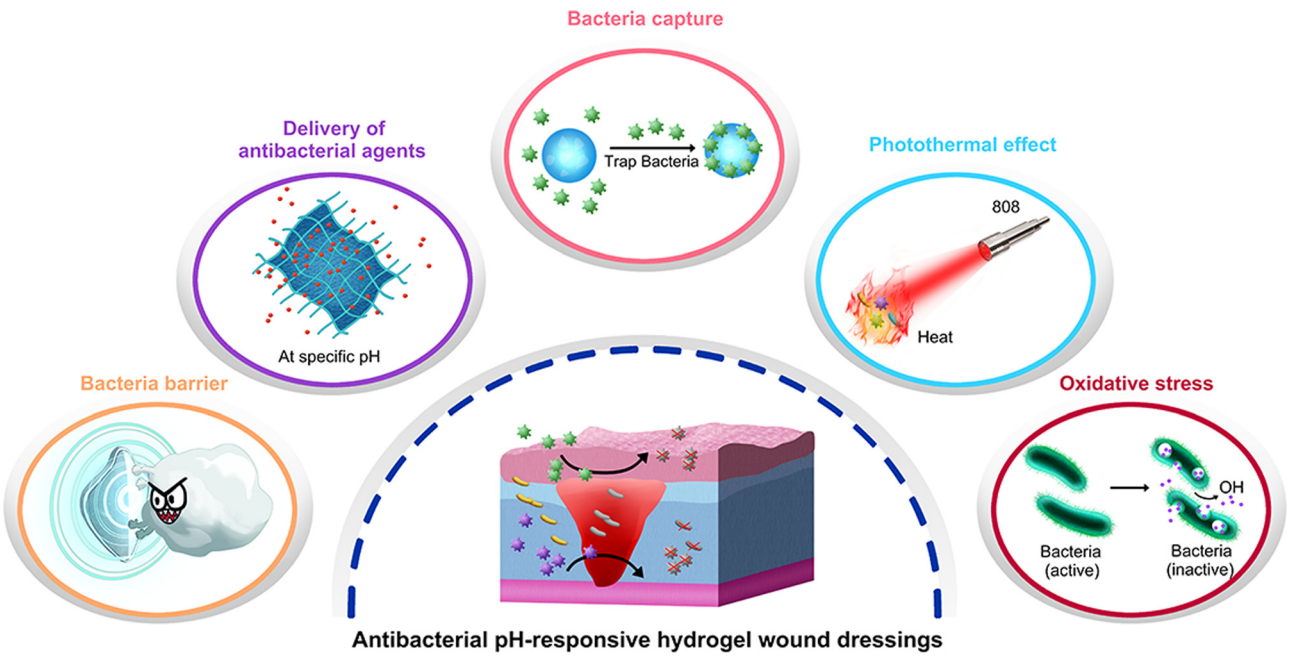

Fig. 3 Antibacterial mechanisms of pH-responsive antibacterial hydrogel wound dressings.

linking agent can reduce the toxicity and cost of supererogatory crosslinkers, and this method is worthy of reference in the pH-responsive design strategy of hydrogels. Meanwhile, the use of adjuvant borneol promoted wound healing.[39] The addition of nanoparticles can also enhance the antibacterial ability, especially metal and nonmetal nanoparticles, such as silver, copper, zinc oxide, silicon, and graphene oxide quantum dots.[34,37,47,77] Mohamed *et al.* added antibiotics to the hydrogel and ZnS nanoparticles simultaneously. According to their results, the minimum inhibitory concentration decreased by 2–16 times after adding ZnS, which effectively increased the ability to inhibit infection.[34] Similar results were also presented by Hu *et al.*, where the addition of silver nanoparticles (AgNPs) significantly improved the antibacterial properties of the hydrogel. Compared with the control group, the hydrogel@AgNPs exhibited a better antibacterial effect (survival rates of 17.8 ± 2.2% for *S. aureus* and 19.7 ± 2.8% for *E. coli*), and the antibacterial ability was increased by more than five times. In addition, deferoxamine was added to promote angiogenesis by increasing the expression of hypoxia-inducible factor-1 alpha and vascular endothelial growth factor.[48] This strategy, which has both antibacterial and growth-promoting properties, was also reported by Shi *et al.*, where a hydrogel loaded with both rifamycin and basic fibroblast growth factor (bFGF) successfully achieved the rapid release of rifamycin and sustained release of bFGF (Fig. 4(a)). The hydrogel not only inhibited the growth of *S. aureus* (Fig. 4(b)) but also promoted cell proliferation and migration, accelerating the wound healing process (Fig. 4(c)).[50] Compared with the antibacterial effect of metal nanoparticles, non-metallic nanoparticles can be used as pH-responsive carriers of antibacterial drugs. Pan *et al.* developed silica nanoparticles that achieved a targeted chlorhexidine release on alkaline wounds and verified their antibacterial ability to both Gram-negative and -positive bacterial pathogens, then silica nanoparticles were further formulated into alginate hydrogels. Based on this strategy, pH-responsive hydrogel wound dressing was prepared.[51] In general, metal and metal oxide nanoparticles are mainly used as antibacterial agents, while non-metallic nanoparticles can be used as drug carriers.

2.2.1.2. Delivery of natural antibacterial agents. At present, the use of antibiotics is the most common approach to treating wound infections. However, their overuse causes long-term side effects and drug resistance. Furthermore, it is risky to only rely on antibiotics to resist future bacterial infections.[78,79] Therefore, many researchers have focused on the use of natural antibacterial compounds to replace the frequent use of antibiotics.[80] In addition, a number of natural antibacterial compounds also possess antioxidant properties that scavenge free radicals, such as honey, resveratrol, curcumin, and tannic acid (TA), which have a synergistic effect on wound healing.[36,40,41,52,53,55,56,58]

Honey is a common antimicrobial and antioxidant agent in food, and according to reports, it has been widely used in the treatment of wounds, including traumatic wounds, surgical incisions, and burns.[81,82] Noori *et al.* synthesized a pH-responsive nanocomposite hydrogel based on chitosan/PVA/nanoclay using a freeze–thaw method. The maximum cumulative release of honey occurred at pH 7, whereas the wound size reduction in the PCMH group was 72.60% compared to that in the control group (55.23%, 6 days). In addition, the antibacterial activity of PCMH reached 99%, demonstrating its potential as an excellent wound dressing.[52] To promote the healing process under acidic wound conditions, Yang *et al.* used

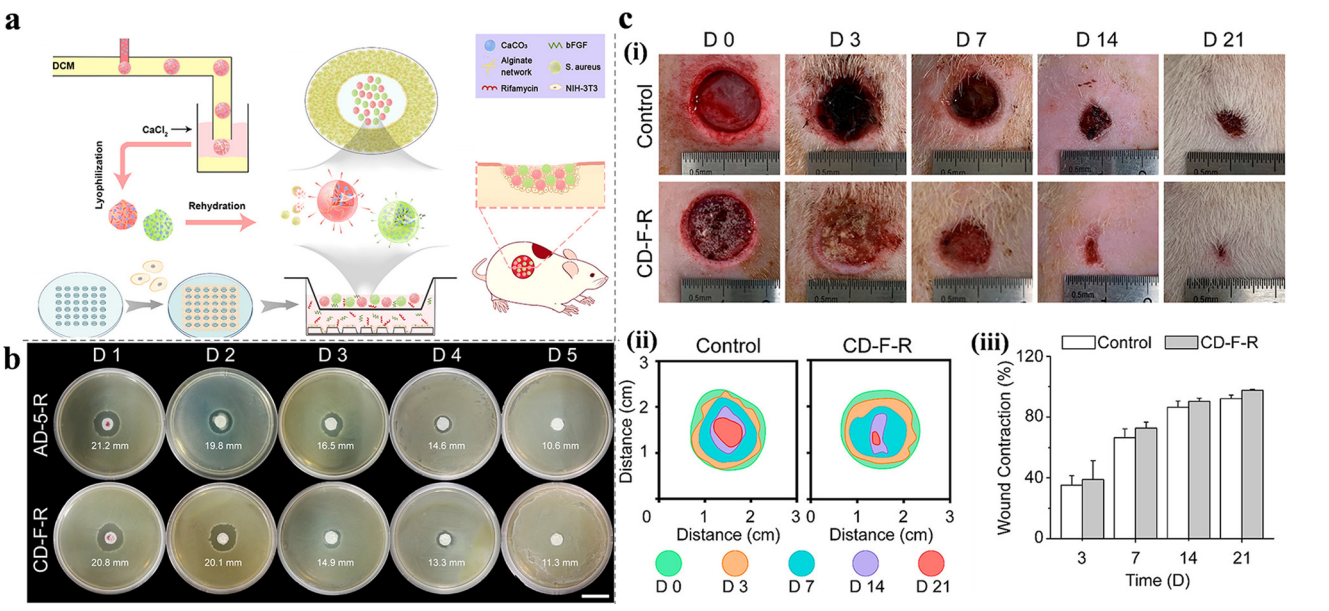

Fig. 4 (a) Preparation process and applications of alginate/$CaCO_3$ composite microparticles. (b) Evaluation of the sustained antibacterial activity of AD-5-R and CD-F-R. (c) *In vivo* performance of the CD-F-R on wound healing. (i) Typical digital images of the wound at predetermined time points. (ii) Traces of wound-bed closure during 21 days. (iii) Wound contraction for control and CD-F-R group. This figure has been reproduced from ref. 50 with permission from American Chemical Society, copyright 2019.

resveratrol (RSV). The natural antibiotic was grafted onto cellulose nanofibrils and poly(vinylalcohol)-borax (PB) to produce a novel pH-responsive hydrogel with antibacterial (Fig. 5(a)), antioxidant and excellent adhesion properties (Fig. 5(c)). The scavenging efficiency of 1,1-diphenyl-2-picrylhydrazyl free radicals (DPPH•) was used to evaluate the antioxidant activity of RSV-grafted cellulose nanofibril (RPC)/PB hydrogels. The groups containing RSV exhibited an increased DPPH• clearance rate, 10–20 times more compared to the groups without RSV, with the rate increasing upon addition of RSV. The inhibition zone method exhibited similar RSV dose-dependent results; the survival rates of RPC/PB-0.2, RPC/PB-0.5, and RPC/PB-0.8 were 29.4, 19.2, and 15.7%, respectively (Fig. 5(b)).[83]

Similar to resveratrol and honey, curcumin is a natural antibacterial and antioxidant agent in food, approved by the Food and Drug Administration. In addition, curcumin has anti-tumor, anti-viral, and anti-inflammatory properties.[84,85] Moreover, curcumin has been reported to accelerate fibroblast migration, collagen deposition, and epithelial regeneration.[36,41,53] Therefore, curcumin is an ideal natural drug for wound dressings owing to its outstanding properties. Qu *et al.* studied the antimicrobial and free radical scavenging properties of QCS/PF hydrogels, as well as their ability to release curcumin in a pH-dependent manner, using *in vitro* experiments. *In vivo* experiments revealed a faster wound-healing rate with less inflammatory infiltration, thicker granulation tissue, higher fibroblast density, and higher collagen deposition (full-thickness skin defect model).[41] Sattari *et al.*, Al-Arjan *et al.* and Nazlı *et al.* also constructed pH-sensitive antibacterial hydrogels loaded with curcumin.[36,53,54] It is worth mentioning that in a previous study, copper oxide and zinc oxide nanoparticles were used cooperatively to enhance the antibacterial properties. The addition of metal nanoparticles to polymer network hydrogels resulted in a more controlled nanoparticle release and increased mechanical toughness of the structure. Notably, in the latter study, the hydrogel showed antibacterial as well as anti-tumor activity. After treatment with curcumin-BSG-4 for 72 h, nearly 87.58% of the U87 cells were non-viable. Such results demonstrate the potential of this wound dressing as a biomaterial for wound care and the treatment of cancer patients.

Tannic acid (TA) is a typical plant-derived hydrolyzable tannin. It is considered an antioxidative, antimicrobial, antiviral, and anti-inflammatory agent.[86,87] It has been used to treat skin ulcers and burns, and its safety has been evaluated by the Food and Drug Administration. Compared with curcumin, resveratrol, and honey, TA itself can additionally act as a crosslinker to form hydrogels because of the interaction between its multiple pyrogallol/catechol groups and macromolecules, forming hydrogen bonds, ionic bonds, coordinate bonds, *etc.*[86,88] Ninan *et al.* developed a novel antibacterial, anti-inflammatory, thermosetting, and pH-sensitive hydrogel based on carboxylate agarose and TA and ionically cross-linked with zinc salts. The hydrogel exhibited antimicrobial activity against *E. coli*, similar to that of gentamicin (the diameters of the inhibition zones of CTZ2 and gentamicin were 8 and 9 mm, respectively). Furthermore, TA presented antimicrobial activity at much lower concentrations than other TA-containing wound dressings. In addition, a nitric oxide (NO) assay was conducted to verify the anti-inflammatory activity of TA, and the results showed that CTZ2-conditioned media could inhibit NO production in a concentration-dependent manner in LPS-activated U-937 cells.[55] Similarly, Ma *et al.* prepared a hydrogel composed

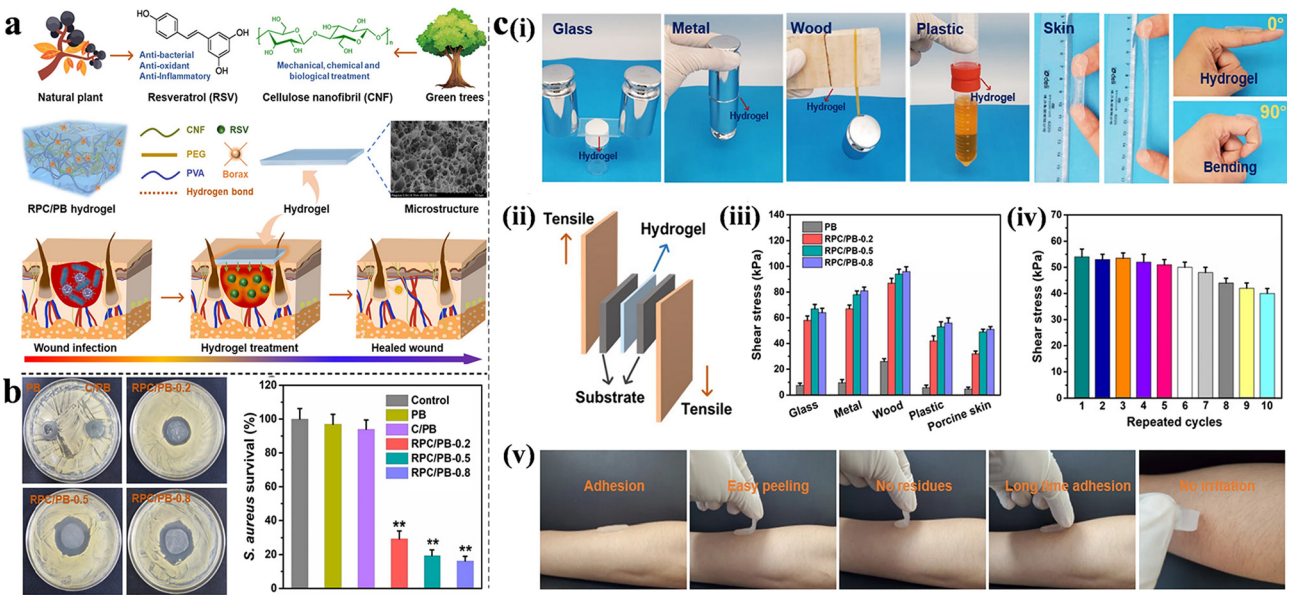

Fig. 5 (a) Schematic illustration, construction and applications of RPC/PB hydrogels in wound healing. (b) Antibacterial activities of the PB, C/PB-0.5 and RPC/PB hydrogels against *S. aureus*. (c) Characterization of adhesion properties and quantitative data analysis of the hydrogel. (i) The adhesion to different surfaces and moved with the finger joint. (ii) Schematic of the hydrogel adhesion measurements. (iii) Adhesive strength to various substrates. (iv) Repeatable adhesion properties on pigskin. (v) No residue after removal on human skin. This figure has been reproduced from ref. 83 with permission from Springer Nature, copyright 2022.

of hydroxypropyl chitin, TA, and ferric ions, with a similar pH-responsive release of TA. Both hydrogels were crosslinked with metal salts, and they showed higher release under acidic conditions.[56] In addition to chemical crosslinking, TA can also form hydrogels *via* physical crosslinking. Ahmadian *et al.* developed a gelatin-GT hydrogel with abundant hydrogen bonding between the functional groups of gelatin (GTU) and TA for the treatment of non-healing chronic and infected wounds (higher TA release at pH 7.4). GTU contains an arginine–glycine–aspartate (RGD) peptide sequence, which provides good cell adhesion and higher hemostatic ability; however, its poor mechanical properties and water sensitivity limit its application. The incorporation of TA overcomes the disadvantages of GTU and endows the hydrogels with inherent anti-inflammatory, antioxidant, and antimicrobial properties. Such a combination is an effective strategy for building multifunctional pH-responsive hydrogels.[58]

It is also an effective way to improve the utilization of natural agents by grafting strategy and then crosslinking with other components to form hydrogels. Magnolol is a natural antioxidant and antibacterial compound, but its poor water solubility leads to low bioavailability. Wang *et al.* synthesized magnolol-grafted-chitosan hydro-chloride *via* EDC/NHS coupling reaction between carboxyl-bearing magnolol derivative and chitosan hydrochloride, and then crosslinked with genipin, forming hydrogel (CSM-H) with dual effects of antibacterial and antioxidant activities. The results showed that the CSM-H hydrogel not only achieved the pH response release of magnolol but also significantly enhanced the antibacterial and antioxidant activities.[59]

2.2.1.3. Other antibacterial mechanisms. Hydrogels are often used as a delivery system for the controlled release of antimicrobial drugs. However, in addition to delivering synthetic/natural antimicrobial agents, hydrogels exhibit various interesting antibacterial mechanisms.

For example, pentaerythritol (PER-TBA) and chitosan CS have been used to synthesize CPT hydrogels with pH responsiveness and intrinsic antibacterial properties *via* the formation of Schiff-base linkages and hydrogen bonds. The antimicrobial mechanisms of CPT hydrogels are summarized as follows: first, the bacteria are inactivated by the interactions between the positively charged CS and negatively charged cell membranes (this antibacterial effect of CS was also confirmed by Khan *et al.* (Fig. 6(a)) and Ding *et al.*)[26,33] Second, the large number of Schiff-base bonds formed by the cross-linking of PER-TBA and CS further enhances the antibacterial properties. The increased PER-TBA dose results in the formation of more Schiff-base bonds, which improves the antimicrobial activity. This was confirmed by the confocal laser scanning microscopy results. In addition, CPT hydrogels are converted to liquid under acidic conditions and can return to a hydrogel state after alkali addition. This pH-responsive morphological change may facilitate the replacement of wound dressings as well as reduce the patients' pain and secondary injuries.[29] Zu *et al.* developed a pH-responsive wound dressing hydrogel composed of transferrin-conjugated copper peroxide nanoparticles (CP@Tf-hy), presenting multiple antimicrobial mechanisms. The positively charged hydrogel carrier is formed by *N*-isopropyl acrylamide, acrylamide, and *N*-[3-(dimethylamino)propyl] methacrylamide *via* free radical polymerization. It can trap and eliminate bacteria with trapping efficiencies of 20.40 and 25.35% against *E. coli* and *B. subtilis*, respectively. Furthermore, under weak acidic conditions, Cu^{2+} is released from CP@Tf-hy, and it decomposes the self-supplied H_2O_2 into $^{\bullet}OH$. The membrane is damaged by both Fenton reactions and GSH oxidation, and 98.78% of *E. coli* and 92.02% of *B. subtilis* are eliminated, confirming a strong antibacterial activity (Fig. 6(b)).[60]

The denaturation of enzymes in bacteria is observed at temperatures above 50 °C, where the proteins and lipids of cell membranes are also damaged, causing bacterial death. Therefore, photothermal therapy has recently emerged as a means of combating bacteria. Hydrogel PEGSD2/GTU showed broad absorption in the near-infrared region, owing to its catechol–Fe^{3+} coordination. After 10 min of NIR irradiation, the highest ΔT was 36.6 °C. Antimicrobial tests showed that after 1 min of NIR irradiation, the killing ratios for *E. coli* and *S. aureus* were 83.9% and 85.0%, respectively.[31] Similarly, Xue *et al.* developed a polysaccharide-based hydrogel to achieve photothermal-assisted bacterial inactivation, using QCS, oxidized hyaluronic acid, photo-thermal agent of poly(styrene-sulfonate), natural antibacterial agent of berberine, and epidermal growth factor. Besides the inherent antibacterial activity of QCS and berberine in hydrogels, the photothermal effect greatly improved the antibacterial properties of hydrogels, reducing the number of colonies of *S. aureus* and *E. coli* to 3.5% and 4.3%.[61] The photothermal effect has attracted much attention in recent years. Hydrogels with photothermal effect can not only help enhance their antibacterial ability, but also broaden the application range of hydrogels by designing temperature sensitivity based on the photothermal effect.

Variations in the pore size of hydrogels may also enhance their antibacterial effect. The PVA-CMC-PEG hydrogel prepared through the freeze–thaw process and phase separation method exhibited different pore sizes from the top to the lower surface, as reported by Li *et al.* During the phase separation process, PEG floated on the surface of the solution, thereby forming larger pores on the top surface. This pore size distribution may strengthen resistance to bacterial infection, with the exact mechanism requiring further investigation.[62]

2.2.2. pH-Responsive pro-healing hydrogel wound dressings. Wound repair is a dynamic and sequential procedure divided into four steps: hemostasis, inflammation, proliferation, and remodeling. At any stage of these processes, wound healing could be affected by a variety of factors, such as infection, humidity, oxygen levels, and diabetes.[20] In addition to their antibacterial effects, pH-responsive hydrogels possess several advantages in regulating wound healing procedures. Therefore, this section focuses on pH-responsive, pro-healing hydrogel wound dressings.

Inflammation plays an important role in wound healing. Appropriate inflammation is indispensable for removing dead tissue and resisting invasive pathogens. However, excessive inflammation leads to congestion and swelling of the tissue around the wound, thus delaying the healing process.[89–91]

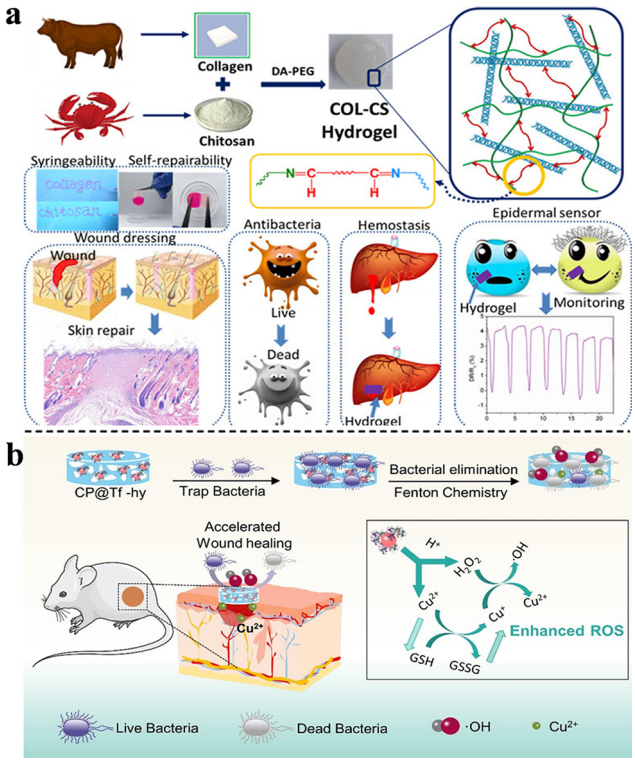

Fig. 6 (a) Construction and applications of COL-CS hydrogels. This figure has been reproduced from ref. 26 with permission from American Chemical Society, copyright 2020. (b) The synthesis of CP@Tf NPs and wound infection treatment *via* bacterial elimination. This figure has been reproduced from ref. 60 with permission from American Chemical Society, copyright 2022.

Therefore, the suppression of excessive inflammation is an effective way to control wound restoration. Nonsteroidal anti-inflammatory drugs can eliminate inflammation by upregulating anti-inflammatory molecules and inhibiting inflammatory pathways.[92] Montaser *et al.* prepared thermosensitive and pH-responsive hydrogels based on PVA/SA-*g*-NIPAM *via* a freeze–thaw technique. Diclofenac sodium was successfully loaded into the mixed solution, and its release was examined *in vitro*. The release of diclofenac sodium was controlled and sustained compared to that of the control group.[63] The umbilical cord stem cell factor (SCF) is an anti-inflammatory bioactive factor secreted by umbilical cord stem cells and has been demonstrated to accelerate the wound healing process by activating M2 macrophages and promoting granulation tissue formation and re-epithelialization. To accelerate wound healing, SCF was loaded into Col/APG hydrogels, and it increased the number of activated M2 macrophages. It promoted angiogenesis and collagen deposition, which displayed a strong pro-healing ability.[30] Therapeutic genetic materials, including DNA, can be loaded into hydrogels to eliminate proteolytic and enzymatic degradation. A PEG-PSMEU copolymer hydrogelator with superior adhesive, mechanical, and bioresorbable properties was successfully developed by Minh *et al.*, and it demonstrated excellent adhesion to various hydrophilic, hydrophobic, and metal substrate surfaces. Quantification of the kinetics of wound closure showed that after one week of treatment, only 30% of the wound area had healed in the control group, whereas 70% had healed in the PEG-PSMEU group and 100% in the polyplex-loaded PEGPSMEU group. The same results were confirmed by hematoxylin and eosin staining, proving the powerful pro-healing properties of PEG-PSMEU and DNA polyplexes.[64] In addition to drug delivery, specific cross-linking bonds may also enhance therapeutic effectiveness on inflammation. Lu *et al.* developed double-network hydrogels based on bioadhesive catechol-chitosan hydrogels. Disulfide bonds formed by the crosslinking of cystamine and *N*,*N*0-bis(a-cryloyl)cystamine enabled redox-responsiveness to the hydrogel; and acetalized cyclodextrin nanoparticles were used to release anti-inflammatory agent Resolvin E1 in a pH-responsive manner. This provided a new strategy for the hydrogel wound dressing to control the inflammation of hard-to-heal wounds and accelerate wound healing.[65]

Apart from common acute and chronic wounds, some special wounds that are difficult to heal have also attracted attention. For example, diabetic chronic wounds, especially diabetic foot ulcers (DFUs), are one of the most serious complications of diabetes, causing long-term pain and even amputation.[93,94] According to the pathophysiology, the two main factors that inhibit DFU healing are diabetic peripheral vasculopathy and neuropathy.[95] pH-responsive hydrogels are effective in healing DFUS and can provide a better method for the treatment of DFUS.[66,67] Li *et al.* were the first to develop a diabetic microenvironment-responsive, self-healing, injectable, and insulin-loaded hydrogel for diabetic wound therapy. In addition, more detailed studies have been conducted to investigate the mechanisms of wound repair, such as re-epithelialization, neovascularization, and the expression of TGF-β1 and VEGF. The hydrogel not only shortened the inflammation phase and enhanced the formation of granulation tissue, neovascular tissue, and epithelium but also improved diabetic peripheral neuropathy, displaying highly promising therapeutic potential for DFUs.[66] Zhao *et al.* synthesized pH and glucose dual-responsive injectable hydrogels that were loaded with insulin and fibroblasts (Fig. 7(a)), which further shortened the healing time (Fig. 7(b)) and enhanced their curative effect against DFUs (Fig. 7(c)). The simultaneous use of bioactive factors and cells is rarely reported in the field of wound dressings, and this may provide an effective strategy for wound dressing.[67] Similarly, Liang *et al.* also constructed pH and glucose dual-responsive hydrogel wound dressings.[68] Different from the above studies, other typical antidiabetic drugs metformin and GO were encapsulated in adhesion-enhanced self-healing easy-removable antibacterial antioxidant conductive hemostasis multifunctional hydrogel wound dressings. This multifunctional hydrogel wound dressing was more suitable for the microenvironment characteristics and wound healing process of diabetic foot, which may have guiding significance for future research. Burns is also a common health problem that is highly susceptible to bacterial infections. Hydrogel wound dressings for burns were prepared by Huang *et al.* by using QCS, oxidized dextran, tobramycin, and polydopamine-coated polypyrrole nanowires. Schiff base bonds

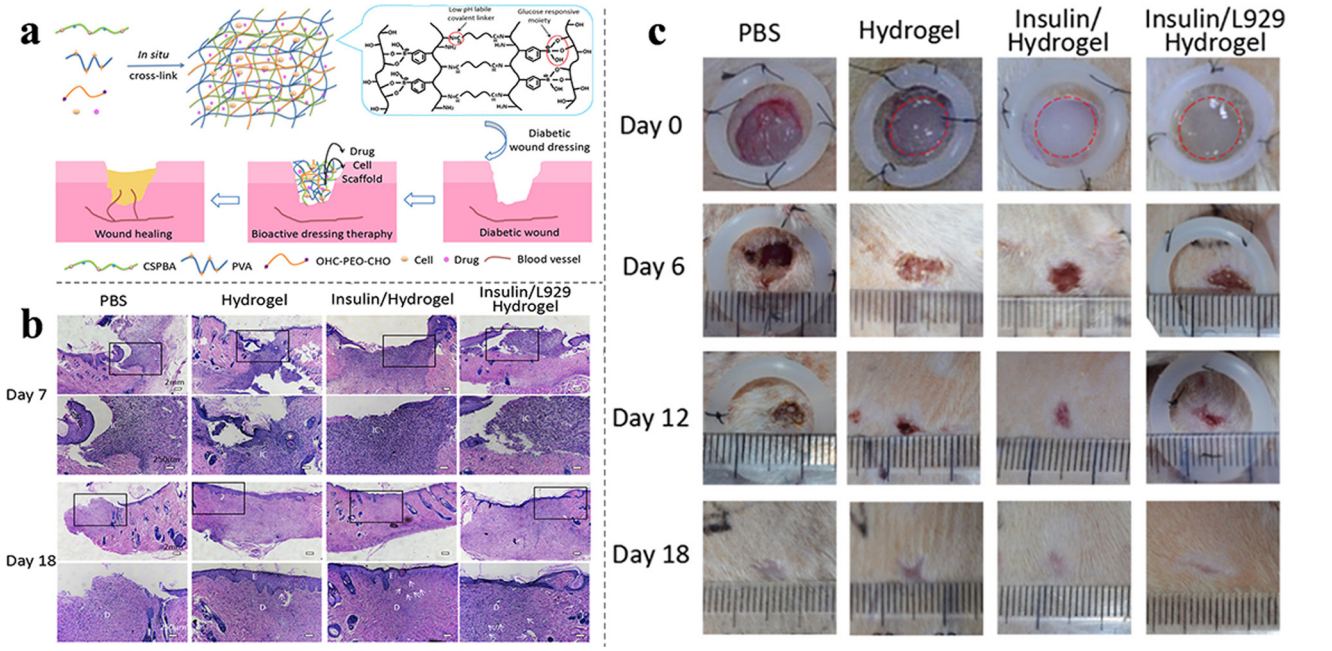

Fig. 7 (a) Synthetic process and applications of insulin- and cell-loaded hydrogels. (b) Images of H&E-stained histopathological sections after 7/18 days of treatment. (c) Wound healing by the hydrogel in STZ-induced diabetic rats. This figure has been reproduced from ref. 67 with permission from American Chemical Society, copyright 2017.

between the oxidized dextran and tobramycin achieved the on-demand release of TOB due to the lower pH caused by the bacteria growth. In addition, the incorporation of polydopamine-coated polypyrrole nanowires endowed the hydrogel with NIR irradiation-assisted bactericidal activity, further enhancing the inhibition of drug-resistant bacteria, and leading to more ideal healing of burn wounds.[24] In general, pH-responsive wound dressings for specific wounds show a trend of multifunctional, through the integration of multiple functions to make the wound healing process more controllable.

3. Other types of pH-responsive wound dressings

pH-Responsive hydrogels are the main type of pH-responsive wound dressings. Other advanced pH-responsive materials include nanofibers,[96] composite films,[97] nanoparticle clusters,[98] and microneedles,[99] each with unique characteristics and advantages for wound healing. In this section, the pH-responsive mechanisms and properties of other pH-responsive materials are discussed, and the relevant information is summarized in Table 2.

Recently, nanofibers have been widely used in biomedical fields, such as tissue engineering, drug delivery, and wound dressings, owing to their large surface area, customizability, biocompatibility, and modifiable properties.[115,116] Thus, based on our investigation, the main application of pH-responsive nanofibers is the prevention or treatment of bacterial infections in wounds. In this section, a summary of the synthetic pathways and properties of pH-responsive nanofibers is presented.

Electrospun membranes are a common type of nanofiber materials. In addition to their primary drug delivery function, their random network arrangement and high porosity (60–90%) are also conducive to cell respiration, wound humidity, and blocking of invasion by external microorganisms.[117] Reshmi *et al.* incorporated NS and poly ε-caprolactone (PCL) by direct electrospinning to form NS@PCL membranes with pH-responsive internal pore sizes. The 25NS@PCL membranes were loaded with gentamicin, and they showed evident bacterial inhibition zones against *S. aure*us and *E. coli*. In addition, 15 days of long-acting antimicrobial activity demonstrated an excellent controlled release effect.[96] Electrospinning technology could realize intelligent drug delivery by adjusting of composition ratio. Liu *et al.* develop CS/PVA/GO nanofibrous membranes with strong antibacterial activity and sustained-release properties. The use of PVA enhanced the electro-spinnability of CS and the addition of 0.1 wt% GO enabled the nanofibrous membrane to a slow-release effect of allicin, thereby achieving the long-term therapeutic effect and improving the bioavailability of allicin.[100] Similarly to hydrogel wound dressings, curcumin is also a potential drug embedded in nanofibers.[35,101–103] For example, PCL/NC membranes synthesized from PCL and NC by Reshmi *et al.* successfully achieved a pH-responsive controlled release of curcumin, further increasing the bioavailability and action time of curcumin.[35] Furthermore, Laura *et al.* prepared three methacrylic acid copolymers (L100-55, S100, and RS100) with different pH-responsiveness to adapt to the environments of different wounds. Specifically, the RIF loaded-L100-55 dressing is designed to prevent infection in intact skin with a pH of 5.5. CHXD-loaded L100-55 dressings are designed for use in infected chronic wounds, whereas the RIF-loaded S100 dressing is appropriate for acute wounds.[104]

Table 2 Summary of other pH-responsive wound dressings

Classification	Application	Composition	Synthetic methods	pH range	pH-Responsive mechanism	Ref.
Nanofibers	Release of gentamycin/vitamin B12	poly ε-caprolactone (PCL), nanostarch (NS)	Electrospinning technique	Higher release at high pH	Slower swelling and erosion of NS particles at low pH	96
	Release of allicin	PVA, GO, CS	Electrospinning technique	Higher release at low pH	The protonation of amino-NH_2 and acetylamino CH_3CONH groups of CS	100
	Release of curcumin	PCL, nanochitosan	Electrospinning technique	Higher release at pH 5.8	Faster swelling and dissolution of NC nanoparticles at pH 5.8	35
	Release of curcumin	PVA, GO, $AgNO_3$	Electrospinning technique	Higher release at pH 5.4	Protonated Ag^+ groups and their interaction with other protonated components in an acidic medium	101
	Release of curcumin	Silk fibroin, CS, $AgNO_3$	Electrospinning technique	Higher release at pH 5.4	The amino and hydroxyl groups in CS and hydroxyl group in curcumin	102
	Release of curcumin	Methyl methacrylate, *N*,*N*-diethylaminoethyl methacrylate	Free-radical polymerization	Higher release at pH 5	—	103
	Release of chlorhexidine, rifampicin, thymol	Methacrylic acid copolymer Eudragit® L100-55, Eudragit® S100, Eudragit® RS100	Electrospinning technique	L100-55 showed high release at pH > 5.5, S100 showed high release at pH > 7, and RS100 showed high release at alkaline conditions	L100-55 dissolves at pH > 5.5, S100 dissolves at pH > 7, and RS100 is pH-independent and slowly erodes and releases the drug	104
	Release of Ag^+	Bacterial cellulose (BC), silver nanoparticles	Chemical reduction	Higher release at acidic conditions	Higher H^+ concentration leads to more Ag oxidation	42
	Release of AgSD	BC	Simple blending method	Higher release at acidic conditions	Higher H^+ concentration causes more SD^- releasing	28
	Release of ICG and DOX	Cellulose nanofiber, dopamine, polyethyleneimine (PEI)	Chemical modification	Higher release at acidic and NIR conditions	CNF-PEI is pH-responsive and CNF-DA fiber is NIR-responsive	105
	Release of ICG and DOX	Cellulose nanocrystal, dopamine, poly(*N*-isopropyl acrylamide), CS	Chemical modification	Higher release at acidic and NIR conditions	The breakage of dynamic imine bonds	106
Composite films						
	Release of neomycin	CS, polyphenolic tannic acid	Chemical crosslinking	Higher release at acidic conditions	High solubility of CS at acidic conditions	97
	Release of epigallocatechin-3-gallate (EGCG)	Hydroxypropyl methylcellulose, EGCG	Formation of hydrogen bonds and hydrophobic interactions	Lower release at basic conditions	Weaker hydrogen bonding at high pH	107
	Release of minocycline	Halloysite nanotube, poly lactide-*co*-glycolide (PLGA), CS	Surface modification	Higher release at basic conditions	Decreased number of $-NH_3^+$ and increased repulsion of $-COO^-$	108
	Release of levofloxacin	Porous silicon, poly(1,7-octadiene), poly(acrylic acid)	Surface modification	Higher release at acidic conditions	The dual plasma polymer layers of poly(1,7-octadiene) and poly(acrylic acid)	109
Nanoparticle clusters	Release of Ag^+	PEG with ortho ester segment and –SH group, $AgNO_3$	Chemical binding	Higher release at acidic conditions	AgNCs hydrolyzed at acidic conditions	98
Microneedles	Smart drug delivery	Stainless steel microneedles with a porous polyactide-*co*-glycolide layer, Eudragit S100	Surface coating	Higher release at basic conditions	Eudragit S100 is dissolvable at alkaline pH and insoluble at acidic pH	99
Sponge	Release of CuO_2	Copper hydroxide and gelatin sponge	Chemical reaction	Higher release at acidic conditions	Fenton reaction	110
	Release of ibuprofen, gentamicin or ciprofloxacin	CS, microspheres	Chemical crosslinking	Cumulative release of gentamicin was higher at pH 4.5 while that of ciprofloxacin was higher at pH 8.0	Different electrostatic interactions between the antibiotics and microspheres	111
Polysaccharide-based dressing	Release of exosomes	Pluronic F127 grafting PEI and aldehyde pullulan	Schiff-base reaction	Higher release at acidic conditions	—	112
Foam	Release of protein drug	Polyurethane foam, alginate-bentonite hydrogel	Vacuum method	Higher release at basic conditions	Weaker crosslinking at high pH	113
	Release of peptide					114

Table 2 (*continued*)

Classification Application	Composition	Synthetic methods	pH range	pH-Responsive mechanism	Ref.
Super-absorbent polymer	Polyaspartic acid and 2-acrylamide-propane sulphonic acid	Free radical polymerization	Higher swell ratios at pH 2 and pH 10	Protonation and dissociation at pH 2–4; protonated $-SO_3H$ and $-COO^-$ groups at pH 7–10	

Cellulose nanofibers are excellent delivery carriers for wound-repairing drugs owing to their high porosity, hydroxyl chemical reaction sites, and machinability. Chen *et al.* prepared pH-responsive CNS-PEI and NIR-responsive CNS-DA nanofibers and then mixed them to form a dual-responsive 3D nanocage structure loaded with ICG and DOX. The pH-activated and NIR-triggered nanocage wound dressings showed high drug delivery capability in the slightly acidic environments of wounds and tumors. In addition, CNF NWD@ICG&DOX, which could induce photothermal therapy, exhibited high antibacterial, antibiofilm, and anti-tumor abilities,[105] a similar study was also carried out in their next work.[106] Shao *et al.* successfully used BC and achieved pH-responsive, controlled release of AgNPs and AgSD. The antibacterial effect of the two BC nanofibers was demonstrated in their studies.[28,42]

Composite films are another type of advanced drug delivery system.[109,115] Huang *et al.* developed a self-assembled multilayer and complex film through the formation of hydrogen bonds and hydrophobic interactions between hydroxypropyl methylcellulose and EGCG. In alkaline environments (near pH 8.0), EGCG transforms from phenol to phenolate ions and then quinone, thereby generating H_2O_2 to kill bacteria. The smart film was able to release antibacterial agents on demand, which is a strategy worth referring to.[107] Chitosan is an excellent film-forming material owing to the presence of amino groups in its polysaccharide backbone, which can ionize at an acidic pH and form a 3D crosslinked film structure. A neomycin-loaded chitosan–tannic acid nanocomposite film was constructed *via* crosslinking. Its bacterial growth inhibition effect and pH-responsive drug release were demonstrated *in vitro*, and its antibacterial activity and drug release profiles were obtained.[97] Furthermore, CS can also be used as a surface modifier to prepare pH-responsive drug delivery system.[108]

Besides hydrogels, nanofibers, and composite membrane materials, the field of pH-responsive wound dressings includes other materials, such as nanoparticle clusters,[98] microneedles,[118] sponges,[110,111] polysaccharide,[112] and foams,[113] which present specific designs and functions. This section is a brief introduction to these materials.

AgNPs are typically used as loading drugs in wound dressings; however, Xie *et al.* employed chemical bonding to endow them with different pH-response characteristics. In particular, Ag nanoparticle clusters (AgNCs) were synthesized using functional polymers containing ortho ester segments as stabilizers (Fig. 8(a)). The ortho ester segment is hydrolyzed under acidic conditions caused by bacterial growth. The AgNCs will then collapse and release individual AgNPs around the bacteria, leading to the death of methicillin-resistant Staphylococcus aureus (MRSA).[98] Microneedles (MNs) are minimally invasive delivery systems that painlessly deliver drugs into subcutaneous tissues and are mainly used for the controlled and sustained release of hydrophilic drugs.[119–121] Ullah *et al.* created a PLGA layer on stainless steel MNs and then coated them with Eudragit S100 (a type of pH-responsive material mentioned above[104]), which enabled the pH-responsiveness of MNs.[99] Gelatin sponge is a frequently-used degradable wound dressing, in the study of Cui *et al.*, CuO_2 was loaded into gelatin sponges. As wound infection occurred (low pH value), copper peroxide was released to kill bacteria through the Fenton reaction producing hydroxyl radicals. Meanwhile, the released Cu^{2+} would also stimulate angiogenesis and collagen deposition, speeding up the wound healing process.[110] In addition to altering their function according to the pH of the wound environment, pH-responsive wound dressings can also act as response elements to

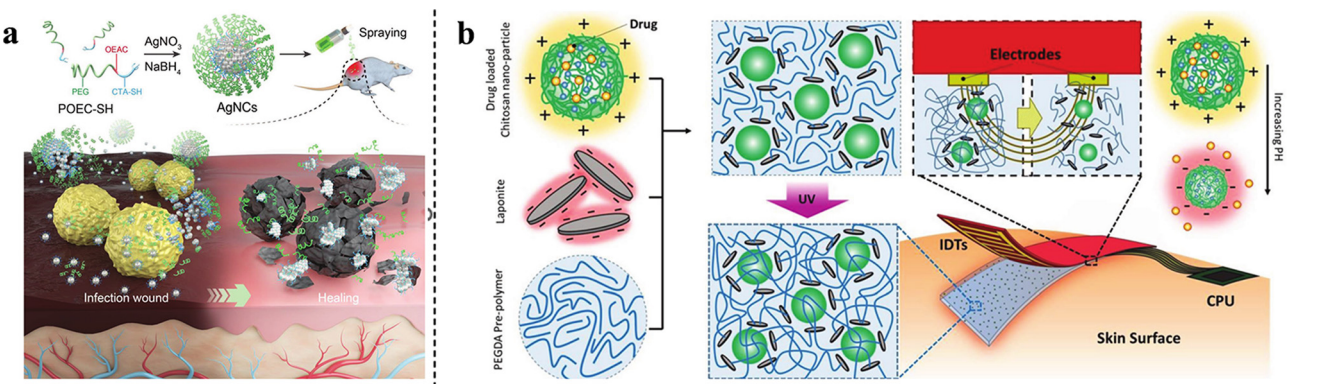

Fig. 8 (a) Synthesis of AgNCs and *in vivo* wound-healing. This figure has been reproduced from ref. 98 with permission from Wiley-VCH, copyright 2020. (b) Schematic representation of the integrated electronic wound dressings. This figure has been reproduced from ref. 122 with permission from Wiley-VCH, copyright 2018.

artificially regulate drug release. Kiaee *et al.* developed an electronic wound dressing consisting of microfabricated electrodes and pH-sensitive poly(ethylene glycol)-diacrylate/LAPONITE® hydrogel, containing drug-loaded chitosan nanoparticles (ChPs). The pH around the anode increases after applying a DC voltage, resulting in drug release from the ChPs; however, under acidic conditions, the release is negligible, achieving controlled drug-release through this strategy (Fig. 8(b)).[122]

4. pH-Responsive wound dressings with monitoring function

Wound healing is a complicated process, with the pH of the wound environment being an important indicator of the wound state.[123] Traditional wound dressings cannot provide information about wound healing, meaning that they must be manually removed or replaced to visually inspect the condition of the wound. This can lead to delayed dressing changes and loss of the opportunity to treat the infection and promote healing.[124] It is therefore necessary to monitor the condition of the wound during treatment. To solve this problem, some researchers have added substances that reflect pH on gauze and fiber pads, such as *Clitoria ternatea* flower extract,[125] red cabbage extract,[126] curcumin,[127] naphthalimide-rhodamine probe,[128] and carbon quantum dots.[129] However, the properties of wound dressings do not change with the addition of pH-displaying agents, and simple gauze or fiber pads are not efficient in meeting the needs of wound healing. Therefore, a combination of multifunctional pH-responsive wound dressings and pH-monitoring functions is essential. pH-responsive wound dressings with monitoring functions not only adjust their properties (antibacterial,[130] hemostatic,[131] and analgesic[132]) according to the condition of the wound but also reflect the state of the wound at the same time, successfully combining diagnosis and treatment, which coincides with the current research trend of nanomedicine.[133] As Fig. 9 shows, the healing process can be observed through the color variation after applying the dressings. The orange arrow indicates that the wound is under normal healing process, while the blue arrow indicates the wound deterioration occurs, warning that the wound needs further treatment.

In this section, the detailed functions of pH-responsive wound dressings with monitoring functions are discussed, and the pH indicators are summarized in Table 3.

Extracts from certain plants act as pH indicators, and the incorporation of these extracts into multifunctional pH-responsive wound dressings is a common and effective strategy to build advanced wound dressings. Elkenawy *et al.* added prodigiosin to gamma-irradiated silver-sulfadiazine-embedded alginate hydrogels. In addition to their antibacterial, antioxidant, and anti-inflammatory properties, they were able to monitor the wound status through the variations in prodigiosin's color. The hydrogel changed from purplish red to yellow in response to bacterial colonization, and the reappearance of purplish red occurred after skin restoration.[134] Similarly, Arafa *et al.* prepared multifunctional chitosan-based hydrogels using red cabbage extract as a natural pH-sensitive indicator.[135] Cui *et al.* prepared smart calcium alginate fibers utilizing alizarin and anthocyanin dyes.[142] Zepon *et al.* and Arafa *et al.* also prepared κC:LBG:CB hydrogel films and hydroxyethyl cellulose hydrogels using cranberry and Curcuma Longa extracts, respectively.[130,136] It is worth mentioning that Wang *et al.* prepared a hydrogel that could be used as a 3D-printed wound dressing ink. They used a multifunctional hydrogel composed of polyacrylamide and chitosan quaternary ammonium salt (HACC-PAM) and added litmus as a pH indicator. The hydrogel displayed excellent antibacterial, hemostatic, and adhesion functions, and its 3D-printable feature enabled it to better assist wounds of different shapes, sizes, and depths. More interestingly, personalized wound management was achieved by utilizing a machine learning model based on the convolutional neural network algorithm, which could recognize and analyze the pH sensing map produced by the litmus in the hydrogel network.[131]

For complex wounds, pH-indicating dyes can be used in combination with other substances that reflect the state of the wound, making the wound assessment more accurate.[124] For example, Zhu *et al.* used phenol red and two glucose-sensing enzymes, glucose oxidase and horseradish peroxidase (HRP), to construct a polycarboxybetaine (PCB) hydrogel and monitor the pH and glucose levels, to achieve better wound management for diabetic ulcers. The color variation (sensitive to changes in the pH of the wound environment due to phenol red) and

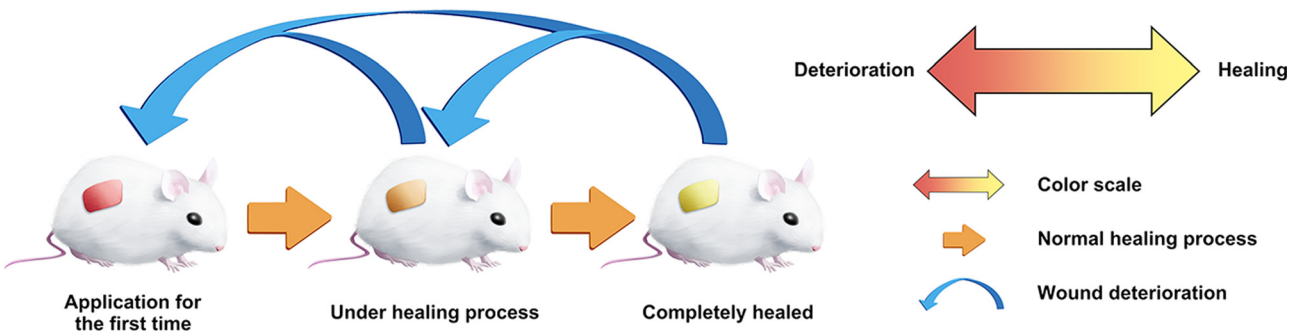

Fig. 9 Schematic of integrated diagnosis and treatment mode of pH-responsive wound dressings with monitoring function.

Table 3 Summary of pH indicators and indication ranges of pH-responsive wound dressings with monitoring functions

Classification	pH indicators	pH indication range	Ref.
Hydrogel	Prodigiosin	Yellow at pH 10 and purplish red at pH 4	134
	Red cabbage extract	pH values 4–9: red for pH < 7 and green for pH > 7	135
	Cranberry extract	Visual color changes at pH 4–9	130
	Curcuma Longa extract	pH values (3–13): yellow for pH ≤ 7 and dark red or reddish-brown for pH > 7	136
	Litmus	Real-time pH monitoring at pH 4–9	131
	Phenol red	Visible color change at pH 4–8	137
	Methacrylate-modified phenol red	Visual color changes at pH 5–9	138
	Cyanine 3 (Cy3) and cyanine 5 (Cy5)	Acidity and alkalinity are indicated by ratios of the fluorescence intensities of Cy5 and Cy3	139
	Ammonium hydrogen citrate carbon dots	Calibration curve of pH values (2–12) and the related fluorescence intensity were plotted	140
	Chitosan–carbon quantum dots and phenol red	Visible color change was observed and the fluorescence intensity normalized curve (5–8) was established	141
Nanofiber	Alizarin dye andanthocyanin dye	Reversible color response at pH 2–11	142
	Bromocresol green	Visual color changes at pH 2–10	132
Nanosheet bandage	Fluorescent magnesium hydroxide nanosheets ($Mg(OH)_2$–NS)	Fluorescence intensity changes at pH 7–10	143

fluorescence signals (generated by glucose oxidation) can be quantified with a spectrophotometer or smartphone for precise measurement (Fig. 10(a)).[137] Liu *et al.* prepared an alginate/polyacrylamide (PAAm) hydrogel using phenol red as the pH indicator. Notably, phenol red was successfully modified with methacrylate, allowing copolymerization with the alginate/PAAm hydrogel matrix. The covalent attachment effectively reduced the dye leaching out of the matrix.[138]

In addition to the combination of pH indicator dyes and multifunctional wound dressings, pH-sensitive fluorescent probes offer a good option. Qiao *et al.* designed a smart hybrid hydrogel capable of monitoring wound infections through pH-responsive fluorescence resonance energy transfer changes in the bacterial environment. Such a hydrogel can provide on-demand therapy for infections *via* NIR-triggered antibiotic release. The pH-monitoring ability was attributed to the energy

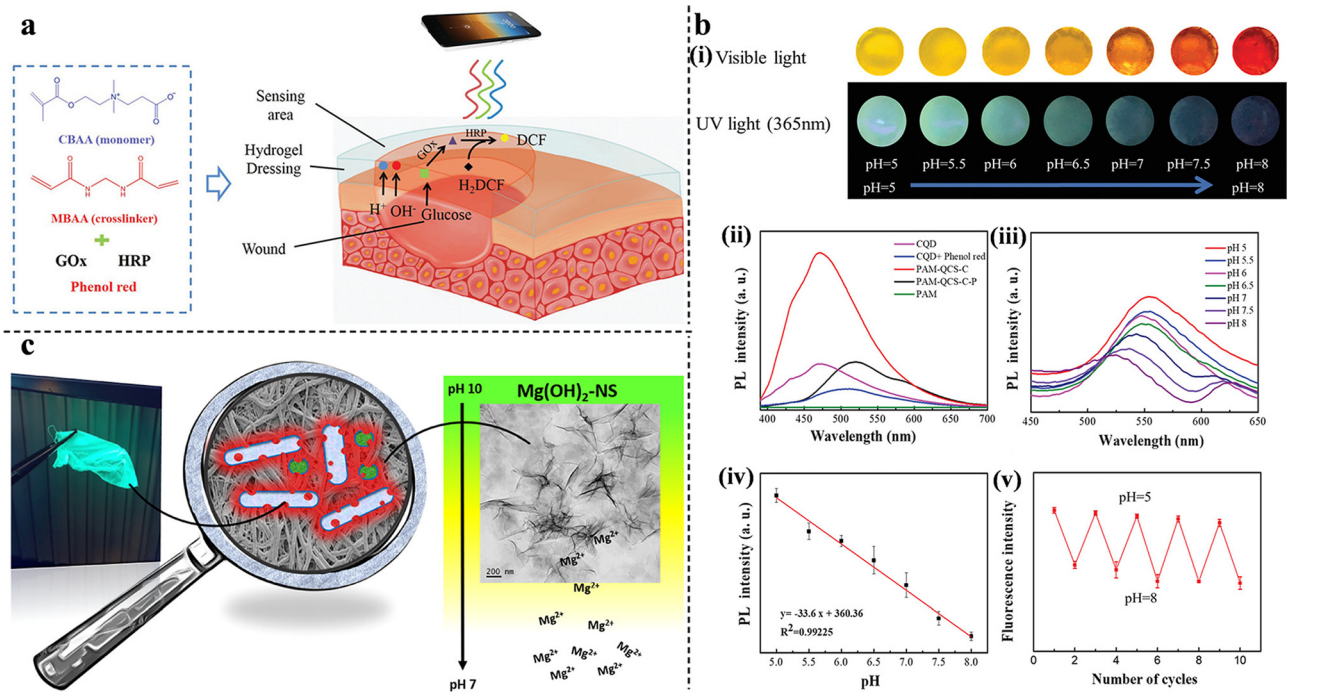

Fig. 10 (a) A schematic representation of the detection of pH and glucose concentration by PCB hydrogels. This figure has been reproduced from ref. 137 with permission from Wiley-VCH, copyright 2019. (b) pH-Sensitivity of PAM-QCS-C-P hydrogels. (i) The color of the hydrogels under sunlight and ultraviolet radiation at different pH values. (ii) The fluorescence intensity of hydrogels, fluorescent hydrogels, and CQD solutions. (iii) The fluorescence emission spectra at different pH values. (iv) The relationship between the fluorescence intensity and pH value. (v) The reversible potential of hydrogels from pH 5–8. This figure has been reproduced from ref. 141 with permission from Wiley-VCH, copyright 2021. (c) Antimicrobial activity and pH-dependent fluorescence quenching of $Mg(OH)_2$–NS electrospun fibers. This figure has been reproduced from ref. 143 with permission from American Chemical Society, copyright 2021.

donor cyanine 3 (Cy3) moiety and the energy acceptor cyanine 5 (Cy5)-loaded silica nanoparticles. Under neutral conditions, stronger Cy5 fluorescence was observed, owing to the fluorescence resonance energy transfer effect between Cy3 and Cy5. When the hydrogels were soaked in an acidic solution, Cy5 was released because of the breakage of the Schiff-base bond between Cy5 and SNP, thereby emitting strong Cy3 fluorescence.[139] Carbon quantum dots (CQDs) have shown promising potential for bioimaging owing to their unique optical properties, biocompatibility, and photoluminescence. Omidi *et al.* added CQDs to chitosan nanocomposite films and successfully monitored the pH of the wound environment (from 4 to 9).[140] Furthermore, to improve the responsiveness and accuracy of wound-state monitoring, Zheng *et al.* synthesized multifunctional double-colorimetry-integrated polyacrylamide-quaternary ammonium chitosan-CQD-phenol red hydrogels. The hybridization of CQDs and phenol red with the hydrogel simultaneously reflected the wound conditions in both ultraviolet and visible light. In addition, real-time remote evaluation can be achieved *via* signals collected by smartphones (Fig. 10(b)).[141] Unlike the previous studies, Truskewycz *et al.* were able to achieve both therapeutic effects and wound status monitoring with a single component. A novel fluorescent magnesium hydroxide nanosheet ($Mg(OH)_2$–NS) was synthesized and incorporated into PCL/polyethylene oxide polymeric fibers. In infected wounds with increased pH, $Mg(OH)_2$–NS would persist and kill bacteria. At decreased pH, when the wound starts to heal, $Mg(OH)_2$–NS would ionize, causing the loss of fluorescence; therefore, the fibers would indicate the pH and predict the wound-healing process (Fig. 10(c)).[143]

5. Conclusions and perspectives

Wound dressings play a significant role in the wound healing process by defending against external microorganisms, maintaining humidity, and releasing drugs. pH-Responsive wound dressings can tune their properties and functions according to the wound status, thereby allowing wounds to heal in a controlled manner and accelerating the healing process. This review summarizes the recent advances in pH-responsive wound dressings, mainly involving three aspects: hydrogels, other materials, and pH-responsive materials. Innovative pH-responsive wound dressings are expected to emerge through rational design and development and achieve excellent clinical performances. Although some preliminary success has been achieved with pH-responsive wound dressings, some challenges remain. Here, we presented the main problems and development trends of pH-responsive wound dressings.

5.1. Multifunctionality

Wound repair is a dynamic and complex process, requiring more than one wound dressing for the entire process. At present, most pH-responsive wound dressings only focus on one or several functions (such as antibacterial, hemostatic, and antioxidant) and do not involve the whole procedure of skin tissue regeneration. Therefore, in the future, pH-responsive wound dressings will develop in the direction of multi-function. Additionally, pH-responsive wound dressings are usually designed based on a single aspect, such as pH-responsive drug release or pH-responsive liquid-to-gel transition. The development of a comprehensive pH-responsive design requires further research.

5.2. Pertinence

Wound types are complex and diverse. The microenvironments of acute wounds, chronic wounds, infected wounds, and special wounds (diabetic ulcers and burns) are significantly different. In addition, the functional emphasis of pH-responsive wound dressings is different for certain wounds. Therefore pH-responsive wound dressings must be prepared depending on the application. Furthermore, pH-responsive wound dressings have been used only in skin wounds, and no studies have been conducted on mucous membranes, especially on the vulnerable oral and nasal mucosa. Mucosal injury is also very common in daily life and medical activities, and the mucosal environment is more complex compared with skin, which makes the development of pH-responsive wound dressings more difficult.

5.3. Integration of diagnosis and treatment

The integration of diagnosis and treatment is a promising strategy for pH-responsive wound dressings. The pH-monitoring function allows physicians to assess the state of the wound while simultaneously monitoring the therapeutic effect of the dressings. Based on the results, it can be decided whether the dressing needs to be replaced or whether further surgical measures should be taken. To date, the pH-monitoring function is mainly attributed to pH indicator dyes that reflect the pH by the variation of visible light/fluorescence; in addition to optical detection, other monitoring mechanisms are awaiting further development.

5.4. Personalization

Personalized customization is also needed in the clinic because of differences in wound characteristics, size, and depth. The wound could be better covered and wrapped by pH-responsive wound dressings that could be trimmed or shaped. 3D printing technology may provide a new strategy to personalize pH-responsive wound dressings. It is reported that 3D-printed hydrogels and nanofibers have been developed, and 3D printing technology will add new vitality to the development of pH-responsive wound dressing in the near future.

Overall, pH-responsive wound dressings have great potential for promoting wound healing owing to their multifunctional merits, such as antibacterial, anti-inflammatory, hemostasis, adhesion, on-demand drug release, and pH monitoring. With the continuous development of interdisciplinary research, it is anticipated that pH-responsive wound dressings will become an important diagnostic and therapeutic tool for wound healing.

Conflicts of interest

There are no conflicts to declare.

Acknowledgements

The authors thank for the financial support of National Science Foundation of China (51803098), Shandong Provincial Natural Science Foundation (ZR2022QE273) and Youth Scientific Research Foundation from the Affiliated Hospital of Qingdao University (QDFYQN202102046). We would like to express our gratitude to Xinqing Fu for the exquisite drawings of Fig. 1, 2, 3 and 9.

References

1 E. M. Tottoli, R. Dorati, I. Genta, E. Chiesa, S. Pisani and B. Conti, *Pharmaceutics*, 2020, **12**, 1–30.
2 H. S. Kim, X. Sun, J. H. Lee, H. W. Kim, X. Fu and K. W. Leong, *Adv. Drug Delivery Rev.*, 2019, **146**, 209–239.
3 K. Kwiecien, A. Zegar, J. Jung, P. Brzoza, M. Kwitniewski, U. Godlewska, B. Grygier, P. Kwiecinska, A. Morytko and J. Cichy, *Cytokine Growth Factor Rev.*, 2019, **49**, 70–84.
4 A. Argenta, L. Satish, P. Gallo, F. Liu and S. Kathju, *PLoS One*, 2016, **11**, 1–16.
5 K. Woo, G. Sibbald, K. Fogh, C. Glynn, D. Krasner, D. Leaper, J. Österbrink, P. Price and L. Teot, *Int. Wound J.*, 2008, **5**, 205–215.
6 A. Popescu and R. S. Salcido, *Adv. Skin Wound Care*, 2004, **17**, 14–22.
7 N. Pazyar, R. Yaghoobi, E. Rafiee, A. Mehrabian and A. Feily, *Skin Pharmacol. Physiol.*, 2014, **27**, 303–310.
8 R. F. Pereira and P. J. Bártolo, *Adv. Wound Care*, 2016, **5**, 208–229.
9 H. Sorg, D. J. Tilkorn, S. Hager, J. Hauser and U. Mirastschijski, *Eur. Surg. Res.*, 2017, **58**, 81–94.
10 S. A. Eming, T. Krieg and J. M. Davidson, *J. Invest. Dermatol.*, 2007, **127**, 514–525.
11 D. Leaper, O. Assadian and C. E. Edmiston, *Br. J. Dermatol.*, 2015, **173**, 351–358.
12 J. Clark and A. Sharp, *Art Sci. Diabetes.*, 2011, **25**, 41–47.
13 G. Power, Z. Moore and T. O'Connor, *J. Wound Care*, 2017, **26**, 381–397.
14 T. Abdelrahman and H. Newton, *Surgery*, 2011, **29**, 491–495.
15 E. A. Kamoun, E. R. S. Kenawy and X. Chen, *J. Adv. Res.*, 2017, **8**, 217–233.
16 M. S. Khil, D. Il Cha, H. Y. Kim, I. S. Kim and N. Bhattarai, *J. Biomed. Mater. Res., Part B*, 2003, **67**, 675–679.
17 Y. Feng, X. Li, Q. Zhang, S. Yan, Y. Guo, M. Li and R. You, *Carbohydr. Polym.*, 2019, **216**, 17–24.
18 R. S. Ambekar and B. Kandasubramanian, *Eur. Polym. J.*, 2019, **117**, 304–336.
19 S. Tavakoli and A. S. Klar, *Biomolecules*, 2020, **10**, 1–20.
20 Y. Liang, J. He and B. Guo, *ACS Nano*, 2021, **15**, 12687–12722.
21 F. Mariani, M. Serafini, I. Gualandi, D. Arcangeli, F. Decataldo, L. Possanzini, M. Tessarolo, D. Tonelli, B. Fraboni and E. Scavetta, *ACS Sens.*, 2021, **6**, 2366–2377.
22 N. Østergaard Knudsen and G. Pommergaard Pedersen, *Curr. Probl. Dermatol.*, 2018, **54**, 143–151.
23 L. A. Wallace, L. Gwynne and T. Jenkins, *Ther. Delivery*, 2019, **10**, 719–735.
24 Y. Huang, L. Mu, X. Zhao, Y. Han and B. Guo, *ACS Nano*, 2022, **16**, 13022–13036.
25 L. A. Schneider, A. Korber, S. Grabbe and J. Dissemond, *Arch. Dermatol. Res.*, 2007, **298**, 413–420.
26 C. Ding, M. Tian, R. Feng, Y. Dang and M. Zhang, *ACS Biomater. Sci. Eng.*, 2020, **6**, 3855–3867.
27 M. A. Qureshi and F. Khatoon, *Polym.-Plast. Technol. Eng.*, 2015, **54**, 573–580.
28 W. Shao, H. Liu, J. Wu, S. Wang, X. Liu, M. Huang and P. Xu, *J. Taiwan Inst. Chem. Eng.*, 2016, **63**, 404–410.
29 L. Fan, Z. He, X. Peng, J. Xie, F. Su, D. X. Wei, Y. Zheng and D. Yao, *ACS Appl. Mater. Interfaces*, 2021, **13**, 53541–53552.
30 L. Zhang, Y. Zhou, D. Su, S. Wu, J. Zhou and J. Chen, *J. Mater. Chem. B*, 2021, **9**, 5887–5897.
31 X. Zhao, Y. Liang, Y. Huang, J. He, Y. Han and B. Guo, *Adv. Funct. Mater.*, 2020, **30**, 1–18.
32 Y. Liang, Z. Li, Y. Huang, R. Yu and B. Guo, *ACS Nano*, 2021, **15**, 7078–7093.
33 M. U. A. Khan, I. Iqbal, M. N. M. Ansari, S. I. A. Razak, M. A. Raza, A. Sajjad, F. Jabeen, M. R. Mohamad and N. Jusoh, *Molecules*, 2021, **26**, 5937.
34 M. M. Ghobashy, A. M. Elbarbary, D. E. Hegazy and N. A. Maziad, *J. Drug Delivery Sci. Technol.*, 2022, **73**, 103399.
35 C. R. Reshmi, P. S. Suja, O. Manaf, P. P. Sanu and A. Sujith, *Int. J. Biol. Macromol.*, 2018, **108**, 1261–1272.
36 W. S. Al-Arjan, M. U. A. Khan, H. H. Almutairi, S. M. Alharbi and S. I. A. Razak, *Polymers*, 2022, **14**, 1949.
37 L. Bonetti, A. Fiorati, A. D'agostino, C. M. Pelacani, R. Chiesa, S. Farè and L. De Nardo, *Gels*, 2022, **8**, 298.
38 S. Du, X. Chen, X. Chen, S. Li, G. Yuan, T. Zhou, J. Li, Y. Jia, D. Xiong and H. Tan, *Macromol. Chem. Phys.*, 2019, **220**, 1–11.
39 X. Fan, L. Yang, T. Wang, T. Sun and S. Lu, *Eur. Polym. J.*, 2019, **121**, 109290.
40 G. Yang, Z. Zhang, K. Liu, X. Ji, P. Fatehi and J. Chen, *J. Nanobiotechnol.*, 2022, 1–16.
41 J. Qu, X. Zhao, Y. Liang, T. Zhang, P. X. Ma and B. Guo, *Biomaterials*, 2018, **183**, 185–199.
42 W. Shao, H. Liu, X. Liu, H. Sun, S. Wang and R. Zhang, *Int. J. Biol. Macromol.*, 2015, **76**, 209–217.
43 M. U. A. Khan, S. Haider, M. A. Raza, S. A. Shah, S. I. A. Razak, M. R. A. Kadir, F. Subhan and A. Haider, *Int. J. Biol. Macromol.*, 2021, **192**, 820–831.
44 M. S. Hosseini and M. R. Nabid, *Int. J. Biol. Macromol.*, 2020, **163**, 336–347.
45 J. Zhu, H. Han, T. T. Ye, F. X. Li, X. L. Wang, J. Y. Yu and D. Q. Wu, *Molecules*, 2018, **23**, 3383.
46 M. U. A. Khan, S. I. Abd Razaq, H. Mehboob, S. Rehman, W. S. Al-Arjan and R. Amin, *Polymers*, 2021, **13**, 3703.
47 Y. Ren, X. Yu, Z. Li, D. Liu and X. Xue, *J. Photochem. Photobiol., B*, 2020, **202**, 111676.

48 C. Hu, L. Long, J. Cao, S. Zhang and Y. Wang, *Chem. Eng. J.*, 2021, **411**, 128564.
49 M. Du, J. Jin, F. Zhou, J. Chen and W. Jiang, *Colloids Surf., B*, 2023, **222**, 113063.
50 M. Shi, H. Zhang, T. Song, X. Liu, Y. Gao, J. Zhou and Y. Li, *ACS Appl. Mater. Interfaces*, 2019, **11**, 22730–22744.
51 F. Pan, G. Giovannini, S. Zhang, S. Altenried, F. Zuber, Q. Chen, L. F. Boesel and Q. Ren, *Acta Biomater.*, 2022, **145**, 172–184.
52 S. Noori, M. Kokabi and Z. M. Hassan, *J. Appl. Polym. Sci.*, 2018, **135**, 1–12.
53 S. Sattari, A. D. Tehrani and M. Adeli, *Polymers*, 2018, **10**, 660.
54 N. S. Bostancı, S. Büyüksungur, N. Hasirci and A. Tezcaner, *Biomater. Adv.*, 2022, **134**, 112717.
55 N. Ninan, A. Forget, V. P. Shastri, N. H. Voelcker and A. Blencowe, *ACS Appl. Mater. Interfaces*, 2016, **8**, 28511–28521.
56 M. Ma, Y. Zhong and X. Jiang, *Carbohydr. Polym.*, 2020, **236**, 116096.
57 M. Fu, Y. Zhao, Y. Wang, Y. Li, M. Wu, Q. Liu, Z. Hou, Z. Lu, K. Wu and J. Guo, *Small*, 2022, 2205489.
58 Z. Ahmadian, A. Correia, M. Hasany, P. Figueiredo, F. Dobakhti, M. R. Eskandari, S. H. Hosseini, R. Abiri, S. Khorshid, J. Hirvonen, H. A. Santos and M. A. Shahbazi, *Adv. Healthcare Mater.*, 2021, **10**, 1–19.
59 M. Wang, H. Huang, C. Huang, S. Liu and X. Peng, *Carbohydr. Polym.*, 2022, **292**, 119643.
60 Y. Zu, Y. Wang, H. Yao, L. Yan, W. Yin and Z. Gu, *ACS Appl. Bio Mater.*, 2022, **5**, 1779–1793.
61 C. Xue, X. Xu, L. Zhang, Y. Liu, S. Liu, Z. Liu, M. Wu and Q. Shuai, *Colloids Surf., B*, 2022, **218**, 112738.
62 Y. Li, C. Zhu, D. Fan, R. Fu, P. Ma, Z. Duan, X. Li, H. Lei and L. Chi, *Int. J. Polym. Mater. Polym. Biomater.*, 2020, **69**, 505–515.
63 A. S. Montaser, M. Rehan and M. E. El-Naggar, *Int. J. Biol. Macromol.*, 2019, **124**, 1016–1024.
64 T. M. D. Le, H. T. T. Duong, T. Thambi, V. H. Giang Phan, J. H. Jeong and D. S. Lee, *Biomacromolecules*, 2018, **19**, 3536–3548.
65 B. Lu, X. Han, D. Zou, X. Luo, L. Liu, J. Wang, M. F. Maitz, P. Yang, N. Huang and A. Zhao, *Mater. Today Bio*, 2022, **16**, 100392.
66 Z. Li, Y. Zhao, H. Liu, M. Ren, Z. Wang, X. Wang, H. Liu, Y. Feng, Q. Lin, C. Wang and J. Wang, *Mater. Des.*, 2021, **210**, 110104.
67 L. Zhao, L. Niu, H. Liang, H. Tan, C. Liu and F. Zhu, *ACS Appl. Mater. Interfaces*, 2017, **9**, 37563–37574.
68 Y. Liang, M. Li, Y. Yang, L. Qiao, H. Xu and B. Guo, *ACS Nano*, 2022, **16**, 3194–3207.
69 M. Li, Y. Liang, J. He, H. Zhang and B. Guo, *Chem. Mater.*, 2020, **32**, 9937–9953.
70 L. Liu, Z. Han, F. An, X. Gong, C. Zhao, W. Zheng, L. Mei and Q. Zhou, *J. Nanobiotechnol.*, 2021, **19**, 1–23.
71 Y. C. Yeh, T. H. Huang, S. C. Yang, C. C. Chen and J. Y. Fang, *Front. Chem.*, 2020, **8**, 1–22.
72 X. Hao, L. Huang, C. Zhao, S. Chen, W. Lin, Y. Lin, L. Zhang, A. Sun, C. Miao, X. Lin, M. Chen and S. Weng, *Mater. Sci. Eng., C*, 2021, **123**, 111971.
73 G. Gao, Y. W. Jiang, H. R. Jia and F. G. Wu, *Biomaterials*, 2019, **188**, 83–95.
74 J. Hu, C. Zhang, L. Zhou, Q. Hu, Y. Kong, D. Song, Y. Cheng and Y. Zhang, *Sci. China Mater.*, 2021, **64**, 1035–1046.
75 Y. Fan, M. Lüchow, Y. Zhang, J. Lin, L. Fortuin, S. Mohanty, A. Brauner and M. Malkoch, *Adv. Funct. Mater.*, 2021, **31**, 2006453.
76 K. Nuutila, J. Grolman, L. Yang, M. Broomhead, S. Lipsitz, A. Onderdonk, D. Mooney and E. Eriksson, *Adv. Wound Care*, 2020, **9**, 48–60.
77 F. Pan, G. Giovannini, S. Zhang, S. Altenried, F. Zuber, Q. Chen, L. F. Boesel and Q. Ren, *Acta Biomater.*, 2022, **145**, 172–184.
78 J. Dai, R. Han, Y. Xu, N. Li, J. Wang and W. Dan, *Bioorg. Chem.*, 2020, **101**, 103922.
79 Y. Yan, X. Li, C. Zhang, L. Lv, B. Gao and M. Li, *Antibiotics*, 2021, **10**, 318.
80 Y. Wang, Y. Yang, Y. Shi, H. Song and C. Yu, *Adv. Mater.*, 2019, **1904106**, 1–21.
81 D. S. Lee, S. Sinno and A. Khachemoune, *Am. J. Clin. Dermatol.*, 2011, **12**, 181–190.
82 J. Yupanqui Mieles, C. Vyas, E. Aslan, G. Humphreys, C. Diver and P. Bartolo, *Pharmaceutics*, 2022, **14**, 1–36.
83 G. Yang, Z. Zhang, K. Liu, X. Ji, P. Fatehi and J. Chen, *J. Nanobiotechnol.*, 2022, **20**, 1–16.
84 A. Giordano and G. Tommonaro, *Nutrients*, 2019, **11**, 2376.
85 S. J. Stohs, O. Chen, S. D. Ray, J. Ji, L. R. Bucci and H. G. Preuss, *Molecules*, 2020, **25**, 1–12.
86 B. Kaczmarek, *Materials*, 2020, **13**, 3224.
87 W. Ge, S. Cao, F. Shen, Y. Wang, J. Ren and X. Wang, *Carbohydr. Polym.*, 2019, **224**, 115147.
88 W. Yan, M. Shi, C. Dong, L. Liu and C. Gao, *Adv. Colloid Interface Sci.*, 2020, **284**, 102267.
89 A. M. Szpaderska and L. A. DiPietro, *Surgery*, 2005, **137**, 571–573.
90 A. C. Lucchini, N. N. Gachanja, A. G. Rossi, D. A. Dorward and C. D. Lucas, *Cells*, 2021, **10**, 1–19.
91 S. Guo and L. A. DiPietro, *J. Dent. Res.*, 2010, **89**, 219–229.
92 Z. Xu, B. Liang, J. Tian and J. Wu, *Biomater. Sci.*, 2021, **9**, 4388–4409.
93 J. Musuuza, B. L. Sutherland, S. Kurter, P. Balasubramanian, C. M. Bartels and M. B. Brennan, *J. Vasc. Surg.*, 2020, **71**, 1433–1446.e3.
94 A. Rathnayake, A. Saboo, U. H. Malabu and H. Falhammar, *World J. Diabetes*, 2020, **11**, 391–399.
95 M. Chang and T. T. Nguyen, *Acc. Chem. Res.*, 2021, **54**, 1080–1093.
96 C. R. Reshmi, P. Sagitha and A. Sujith, *Cellulose*, 2022, **29**, 427–443.
97 F. Chowdhury, S. Ahmed, M. Rahman, M. A. Ahmed, M. D. Hossain, H. M. Reza, S. Y. Park and S. M. Sharker, *Mater. Today Commun.*, 2022, **31**, 103310.
98 X. Xie, T. C. Sun, J. Xue, Z. Miao, X. Yan, W. W. Fang, Q. Li, R. Tang, Y. Lu, L. Tang, Z. Zha and T. He, *Adv. Funct. Mater.*, 2020, **30**, 1–10.

99 A. Ullah, M. Jang, H. Khan, H. J. Choi, S. An, D. Kim, Y. R. Kim, U. K. Kim and G. M. Kim, *Sens. Actuators, B*, 2021, **345**, 130441.
100 Y. Liu, R. Song, X. Zhang and D. Zhang, *Int. J. Biol. Macromol.*, 2020, **161**, 1405–1413.
101 E. Rahmani, M. Pourmadadi, N. Zandi, A. Rahdar and F. Baino, *Micromachines*, 2022, **13**, 1847.
102 P. Heydari Foroushani, E. Rahmani, I. Alemzadeh, M. Vossoughi, M. Pourmadadi, A. Rahdar and A. M. Díez-Pascual, *Nanomaterials*, 2022, **12**, 3426.
103 M. Gorji, D. Zarbaf, S. Mazinani, A. S. Noushabadi, M. A. Cella, A. Sadeghianmaryan and A. Ahmadi, *J. Biomater. Sci., Polym. Ed.*, 2022, **0**, 1–21.
104 L. Miranda-Calderon, C. Yus, G. Landa, G. Mendoza, M. Arruebo and S. Irusta, *Int. J. Pharm.*, 2022, **624**, 122003.
105 R. Chen, C. Zhao, Z. Chen, X. Shi, H. Zhu, Q. Bu, L. Wang, C. Wang and H. He, *Biomaterials*, 2022, **281**, 121330.
106 Y. He, R. Chen, C. Zhao, Q. Lu, Z. Chen, H. Zhu, Q. Bu, L. Wang and H. He, *ACS Appl. Mater. Interfaces*, 2022, 51630–51644.
107 T. W. Huang, H. T. Lu, Y. C. Ho, K. Y. Lu, P. Wang and F. L. Mi, *Mater. Sci. Eng., C*, 2021, **118**, 111396.
108 A. Mohebali and M. Abdouss, *Int. J. Biol. Macromol.*, 2020, **164**, 4193–4204.
109 R. B. Vasani, E. J. Szili, G. Rajeev and N. H. Voelcker, *Chem. – Asian J.*, 2017, **12**, 1605–1614.
110 H. Cui, M. Liu, W. Yu, Y. Cao, H. Zhou, J. Yin, H. Liu, S. Que, J. Wang, C. Huang, C. Gong and G. Zhao, *ACS Appl. Mater. Interfaces*, 2021, **13**, 26800–26807.
111 A. B. Ozdabak-Sert, B. Sen and F. N. Kok, *J. Appl. Polym. Sci.*, 2019, **136**, 1–10.
112 M. Wang, C. Wang, M. Chen, Y. Xi, W. Cheng, C. Mao, T. Xu, X. Zhang, C. Lin, W. Gao, Y. Guo and B. Lei, *ACS Nano*, 2019, **13**, 10279–10293.
113 S. T. Oh, W. R. Kim, S. H. Kim, Y. C. Chung and J. S. Park, *Fibers Polym.*, 2011, **12**, 159–165.
114 S. Sharma, A. Dua and A. Malik, *J. Polym. Res.*, 2017, **24**, 1–8.
115 S. Chen, J. V. John, A. McCarthy and J. Xie, *J. Mater. Chem. B*, 2020, **8**, 3733–3746.
116 R. S. Ambekar and B. Kandasubramanian, *Eur. Polym. J.*, 2019, **117**, 304–336.
117 M. Abrigo, S. L. McArthur and P. Kingshott, *Macromol. Biosci.*, 2014, **14**, 772–792.
118 A. Ullah, M. Jang, H. Khan, H. J. Choi, S. An, D. Kim, Y. R. Kim, U. K. Kim and G. M. Kim, *Sens. Actuators, B*, 2021, **345**, 130441.
119 J. H. Jung and S. G. Jin, *J. Pharm. Invest.*, 2021, **51**, 503–517.
120 K. Ahmed Saeed AL-Japairai, S. Mahmood, S. Hamed Almurisi, J. Reddy Venugopal, A. Rebhi Hilles, M. Azmana and S. Raman, *Int. J. Pharm.*, 2020, **587**, 119673.
121 R. Jamaledin, C. K. Y. Yiu, E. N. Zare, L. N. Niu, R. Vecchione, G. Chen, Z. Gu, F. R. Tay and P. Makvandi, *Adv. Mater.*, 2020, **32**, 1–29.
122 G. Kiaee, P. Mostafalu, M. Samandari and S. Sonkusale, *Adv. Healthcare Mater.*, 2018, **7**, 1–8.
123 S. L. Percival, S. McCarty, J. A. Hunt and E. J. Woods, *Wound Repair Regen.*, 2014, **22**, 174–186.
124 M. S. Brown, B. Ashley and A. Koh, *Front. Bioeng. Biotechnol.*, 2018, **6**, 1–21.
125 K. Kiti, C. Thanomsilp and O. Suwantong, *Microchem. J.*, 2022, **177**, 107277.
126 O. Alaysuy, R. M. Snari, A. A. Alfi, A. M. Aldawsari, S. Abu-Melha, M. E. Khalifa and N. M. El-Metwaly, *Int. J. Biol. Macromol.*, 2022, **211**, 390–399.
127 N. Pan, J. Qin, P. Feng, Z. Li and B. Song, *J. Mater. Chem. B*, 2019, **7**, 2626–2633.
128 J. Zhou, B. Jiang, C. Gao, K. Zhu, W. Xu and D. Song, *Sens. Actuators, B*, 2022, **355**, 131310.
129 P. Yang, Z. Zhu, T. Zhang, W. Zhang, W. Chen, Y. Cao, M. Chen and X. Zhou, *Small*, 2019, **15**, 1–11.
130 K. M. Zepon, M. M. Martins, M. S. Marques, J. M. Heckler, F. Dal Pont Morisso, M. G. Moreira, A. L. Ziulkoski and L. A. Kanis, *Carbohydr. Polym.*, 2019, **206**, 362–370.
131 L. Wang, M. Zhou, T. Xu and X. Zhang, *Chem. Eng. J.*, 2022, **433**, 134625.
132 M. Kurečič, T. Maver, N. Virant, A. Ojstršek, L. Gradišnik, S. Hribernik, M. Kolar, U. Maver and K. S. Kleinschek, *Cellulose*, 2018, **25**, 7277–7297.
133 P. Tan, X. Chen, H. Zhang, Q. Wei and K. Luo, *Semin. Cancer Biol.*, 2023, **89**, 61–75.
134 N. M. Elkenawy, H. M. Karam and D. S. Aboul-magd, *Int. J. Biol. Macromol.*, 2022, **211**, 170–182.
135 A. A. Arafa, A. A. Nada, A. Y. Ibrahim, P. Sajkiewicz, M. K. Zahran and O. A. Hakeim, *Int. J. Biol. Macromol.*, 2021, **182**, 1820–1831.
136 A. A. Arafa, A. A. Nada, A. Y. Ibrahim, M. K. Zahran and O. A. Hakeim, *Eur. Polym. J.*, 2021, **159**, 110744.
137 Y. Zhu, J. Zhang, J. Song, J. Yang, Z. Du, W. Zhao, H. Guo, C. Wen, Q. Li, X. Sui and L. Zhang, *Adv. Funct. Mater.*, 2020, **30**, 1–9.
138 L. Liu, X. Li, M. Nagao, A. L. Elias, R. Narain and H. J. Chung, *Polymers*, 2017, **9**, 558.
139 B. Qiao, Q. Pang, P. Yuan, Y. Luo and L. Ma, *Biomater. Sci.*, 2020, **8**, 1649–1657.
140 M. Omidi, A. Yadegari and L. Tayebi, *RSC Adv.*, 2017, **7**, 10638–10649.
141 K. Zheng, Y. Tong, S. Zhang, R. He, L. Xiao, Z. Iqbal, Y. Zhang, J. Gao, L. Zhang, L. Jiang and Y. Li, *Adv. Funct. Mater.*, 2021, **31**, 1–13.
142 L. Cui, J. Jing Hu, W. Wang, C. Yan, Y. Guo and C. Tu, *Cellulose*, 2020, **27**, 6367–6381.
143 A. Truskewycz, V. K. Truong, A. S. Ball, S. Houshyar, N. Nassar, H. Yin, B. J. Murdoch and I. Cole, *ACS Appl. Mater. Interfaces*, 2021, **13**, 27904–27919.

